2010

Reconfiguration of power networks based on graph-theoretic algorithms

Juan Li
Iowa State University

Reconfiguration of power networks based on graph-theoretic algorithms

by

Juan Li

A dissertation submitted to the graduate faculty

in partial fulfillment of the requirements for the degree of

DOCTOR of PHILOSOPHY

Major: Electrical Engineering

Program of Study Committee:
Chen-Ching Liu, Major Professor
Manimaran Govindarasu
Venkataramana Ajjarapu
Dionysios Aliprantis
Dan Nordman

Iowa State University

Ames, Iowa

2010

TABLE OF CONTENTS

LIST OF FIGURES

LIST OF TABLES

ACKNOWLEDGEMENT

My foremost and tremendous appreciation goes to my major professor, Dr. Chen-Ching Liu, who provided me with his continuous support, inspirations, challenges and encouragement during my research work. This dissertation work could not have been completed without his insightful and invaluable technical advice. The precious experience of working with him as a teaching assistant and as a research assistant on a variety of projects will have a profound influence on my future career development.

I would also like to express my sincere thanks to Prof. Venkataramana Ajjarapu, Prof. Manimaran Govindalasu, Prof. Dionysios Aliprantis and Prof. Dan Nordman for serving on my committee. Their valuable feedback and suggestions were essential in improving the dissertation.

I am very grateful to my parents Zhen-Ju Zheng and Quan-Xi Li, my beloved husband, Nanpeng Yu, for their endless support and love as always.

The research work in this dissertation was supported by Power Systems Engineering Research Center (PSERC) and Pacific Northwest National Laboratory (PNNL). Special thanks go to Dr. Kevin Schneider, Mr. Dave Chassin and Dr. Frank Tuffner at PNNL for their valuable comments and technical support.

Last but not least, I would like to thank all my dear friends in the power group at Iowa State University. Their friendship, encouragement and help made my stay in Ames an enjoyable memory.

ABSTRACT

The intentional area partitioning and automated distribution system restoration are two important "Smart Grid" technologies to enhance the robustness of a power network and improve the system reliability. In this dissertation, the research work is focused on deriving and implementing efficient graph-theoretic algorithms to analyze and solve such two real-world problems in power systems as follows.

In response to disturbances, a self-healing system reconfiguration that splits a power network into self-sufficient islands can stop the propagation of disturbances and avoid cascading events. An area partitioning algorithm that minimizes both real and reactive power imbalance between generation and load within islands is proposed. The proposed algorithm is a smart grid technology that applies a highly efficient multilevel multi-objective graph partitioning technique. The simulation results obtained on a 200- and a 22,000- bus test systems indicate that the proposed algorithm improves the voltage profile of an island after the system reconfiguration compared with the algorithm that only considers real power balance. In doing so, the algorithm maintains the computational efficiency.

The distribution system restoration is aimed at restoring loads after a fault by altering the topological structure of the distribution network by changing open/closed states of some tie switches and sectionalizing switches in the distribution system. A graph-theoretic distribution system restoration strategy that maximizes the amount of load to be restored and minimizes the number of switching operations is developed. Spanning tree based algorithms are applied to find the candidate restoration strategies. Unbalanced three-phase power flow calculation is performed to guarantee that the proposed system topology meets all electrical

and operational constraints. Simulation results obtained from realistic feeder models demonstrate the effectiveness of the proposed approach.

CHAPTER 1. INTRODUCTION

1.1 Smart Grids & Self-Healing Power Networks

Recent blackouts in North America, Europe, and other regions in the world highlight the need to develop smart power networks with self-healing features that could respond to vulnerable operating conditions and prevent catastrophic outages. A self-healing smart grid, which has better situational awareness and autonomous control capabilities against cascaded events, has been envisioned by the U.S. Department of Energy [1]. The ability to "self-heal" by anticipating and responding to system disturbances is an important characteristic of the smart grid in the future [2]. Self-healing, as the immune system of the smart grid, is aimed at detecting patterns that are precursors to disturbances and limiting the impact of the events to the smallest load area by preventive/corrective actions before/after disturbances [3]. A self-healing smart grid is expected to reduce the frequency and magnitude of power outages, minimize the system restoration time, thereby enhancing customer satisfaction and the system reliability.

1.1.1 "Self-Healing" Power Transmission Network

At the transmission level, the "Self-healing" smart grid is envisioned to take advantage of available modern technologies in transforming the current grid to one with better capabilities for situational awareness and autonomous controls against component failures to enhance reliability and increase resiliency [2]. Several technologies have been applied to equip today's transmission power network with "self-healing" features. Wide-Area monitoring and control has received great attention. The synchronized phasor measurement technology brings many potential applications to enhance the system situational awareness capabilities, including phasor angle instability prediction [4], dynamic voltage stability monitoring [5] and low-frequency oscillation monitoring [6]. A conceptual design of the Strategic Power Infrastructure Defense (SPID) system has been developed [7]. The SPID system is aimed at prevention of the wide area grid outages against cascaded events caused by a series of problems including short circuits and equipment failures. "Self-Healing" control actions, such as special protection schemes (SPSs) and remedial action schemes (RASs) against cascading failures have been equipped and incorporated in power systems [8]. Some controlled system islanding schemes have been incorporated into SPSs, such as the controlled islanding between Alberta and the Western Interconnection in North America [9] as well as the Automatic System Separation (AS) in Russia [10]. Another important self-healing control action is load shedding. An adaptive load shedding method is proposed in [11].

A major challenge for the future self-healing control actions at the transmission level is to evaluate the system vulnerable operating conditions and response to major disturbances in an on-line environment. Advanced communication and information technologies are needed to enable an IT infrastructure that provides grid-wise coordinated monitoring and fast control capabilities [12].

1.1.2 "Self-Healing" Power Distribution System

At the distribution level, distribution automation (DA) technologies are being deployed to enable the distribution system's "Self-healing" capabilities. The main functions of DA consist of real-time monitoring, control and automated operation of distribution feeders. Through a well-designed DA system, a distribution system is able to optimize its operation and improve its reliability in a number of areas, e.g.,

- Expediting fault detection, fault isolation and service restoration
- Intelligently reconfiguring distribution network to reduce losses
- Improving power quality by remote voltage and power factor control
- Increasing infrastructure reliability
- Reducing operating and maintenance costs
- Enhancing customer satisfaction

With the growing needs of renewable energy and increasing penetration of distributed generations, DA applications should be extended to coordinate with new customer applications, such as demand response management. Today most DA and substation automation (SA) systems are applied at a local level using local information for decision-making and control [3]. Hence, the network reconfiguration for restoration purpose is limited to neighboring feeders. With the advent of advanced high-speed communication and IT technologies, a more advanced DA system involving global control operations in a larger area with multiple feeders and substations is expected.

1.2 Motivation

A power system undergoing large disturbances may become unstable leading to an uncontrolled system separation. Unlike an uncontrolled system separation, an intentional and controlled system separation can balance generation and load within the islands. Therefore, the system frequency within the islands can be regulated within allowable limits and the islands formed by controlled system separation would be less prone to a system collapse. If an intentional system separation scheme is conducted appropriately, the impact of the disturbance can be contained in a smaller area. As a result, cascading failures and large-scale blackouts can be avoided [13]. Such a flexible power network configuration by partitioning is a "Smart Grid" technology to improve the robustness of a power infrastructure and enhance the system reliability.

The automated distribution system restoration is also an important "Smart Grid" technology to improve the distribution system reliability. Distribution restoration is an important task to restore loads after a fault by altering the topological structure of the distribution network while meeting electrical and operational constraints. Such a network reconfiguration process is achieved by changing open/closed states of a number of tie-switches and sectionalizing switches in the distribution system. An efficient distribution system restoration strategy to quickly determine and optimize restoration plans can significantly reduce the overall customer outage time, thereby enhancing customer satisfaction and quality of the power supplying service. Recent developments of the Intelligent Electronic Devices (IEDs) for protection, control, and communication make it possible to realize the automated distribution system restoration in a real time environment.

Due to the large size and nonlinearity of power systems, both the transmission system reconfiguration and the distribution system restoration problem are large scale and complex optimization problems. The transmission and distribution networks can be represented by a graph of G (V, E) that contains a set of vertices, V, and a set of edges, E. Therefore, both the transmission system reconfiguration and the distribution system restoration problem can be formulated as problems of identifying the desired graph topology subject to a variety of complex constraints.

In the research work presented in this dissertation, significant results have been obtained in deriving and implementing efficient graph-theoretic algorithms to analyze and solve the real-world problems in power systems. The main reasons for the application of graph theoretic methods in this research include: (i) power networks are naturally modeled as graphs, (ii) topology constraints of power networks can be handled by graph theoretic algorithms, (iii) well designed graph theoretic algorithms provide better solutions than local suboptimal solutions, (iv) well developed and efficient graph-theoretic algorithms are powerful tools for the solutions of combinatorial problems, (v) the data structure for graph and network programming techniques can facilitate the implementation of graph theoretic algorithms.

1.3 Literature Review

1.3.1 Reconfiguration of Power Transmission Network

System reconfiguration of the transmission network that intentionally partitions a power network into self-sufficient islands is an emergency control to stop the propagation of disturbances and avoid cascading failures. Several efforts have been made to develop an efficient area-partitioning algorithm that can partition the power network into k-disjoint areas via minimizing the generation load imbalance in each area.

A few methods have been proposed to determine the optimal islanding configuration. A three-phase method utilizing ordered binary decision diagrams (OBDDs) to find proper islanding strategies is proposed in [14]. An automatic islanding approach that determines the islands from the identified slowly varying coherent groups of generators is reported in [15]. A partition strategy using minimal cut sets with minimum net flow is proposed in [16]. A spectral k-way partition algorithm is provided in [7]. Based on the generator grouping information, a two-step partitioning approach including graph simplification and multilevel k-way partition is presented in [17] and demonstrated on the August 14, 2003 blackout scenario [13]. An efficient integrated islanding cut set identification algorithm is developed in [18].

Reconfiguration of power transmission network is an important part of the future grid protection and control actions. However, most of existing power system reconfiguration schemes determine the system partitioning solution based on off-line studies that may not reflect the real time system operating condition and may lead to an inappropriate partitioning plan.

1.3.2 Reconfiguration of Power Distribution System

Researchers have applied a variety of techniques to address the distribution system restoration problem from various perspectives. Liu et al. [19] incorporated operator's knowledge and experience into an expert system to assist the restoration process. Aoki et al. [20] formulated the distribution restoration problem as an optimization problem and developed a dual effective gradient method for the solution. Hsu and Kuo [21] proposed a fuzzy reasoning approach. Fukuyama et al. [22] developed a parallel genetic algorithm. Zhou et al. [23] combined optimization techniques with heuristic rules and fuzzy logic. Lee et al. [24] applied a fuzzy logic approach to combine multiple conflicting objectives of the distribution system restoration problem into a single objective. Miu et al. [25] provided a multi-tier service restoration algorithm to determine the switching operations and capacitor control actions. Chen et al. [26] extended a rule based system to incorporate colored Petri net modeling, while Hsiao and Chien [27] combined the fuzzy based approach with genetic algorithms. Nagata and Sasaki [28] identified a sub-optimal configuration after faults with a multi-agent based approach. Lim et al. [29] analyzed the distribution restoration problem with multiple faults using a fuzzy decision-making method. Tsai [30] presented an object-oriented expert system that considers load variations. Carvalho et al. [31] approached the distribution restoration problem by solving two optimization sub-problems with genetic algorithms and dynamic programming. Pérez-Guerrero and Heydt solved the distribution restoration problem with dynamic programming [32] and Lagrangian Relaxation [33].

The above developed algorithms for the distribution restoration problem can be divided into three divisions, rule-based approaches, optimization approaches, and heuristic search approaches. There are also algorithms that combine more than one of above approaches.

The rule-based system method that consists of rules built with the experience of operators provides a natural way to incorporate the human knowledge. Such a rule-based approach is adopted by industry and it tends to provide local optimal or sub-optimal solution. A software tool has to be tailored for a specific distribution system in order to capture the system specific characteristics. The maintenance and support of such a specialized software tool can be a major task [34].

The conventional optimization methods for distribution system restoration include mathematical programming, mixed integer programming, dynamic programming, and Lagrangian Relaxation. These optimization technologies require adequate and precise models to achieve the global optimality. For the traditional optimization approaches, it is difficult to include the objective function as well as electrical and operating constraints in the formulation of a complex distribution network model. As a result, optimization methods may not guarantee a feasible sequence of switching operations that satisfy network and reliability constraints. Heuristic optimization methods, such as genetic algorithm (GA), tabu search, and simulated annealing (SA) are single point neighborhood search based methods, which cannot guarantee the global optimality [31].

A heuristic search approach is based on an understanding of the system and operation characteristics of a distribution network, such as radial configuration, multiple alternative supply feeders, and operational experience. A well-designed heuristic approach can be used to determine feasible solutions without violating network and reliability constraints, but it does not guarantee a global optimal solution.

1.3 Contributions of This Dissertation

The primary objective of this research is to derive and implement efficient, graph-theoretic algorithms to analyze and solve the transmission system reconfiguration and the distribution system restoration problems. The main contributions of this dissertation are as follows,

- This dissertation is believed to be the first to propose an intentional area partitioning algorithm considering both real and reactive power balance. The proposed area partitioning algorithm not only regulates the system frequency within allowable limits by minimizing real power imbalance between generation and load, but also avoids the low voltage profile after the system separation by providing a more balanced reactive power supply and demand in each island.

- ✧ A graph theory based distribution system restoration strategy that minimizes the outage and number of switching operations is developed. The proposed spanning tree search algorithm is a new application for distribution feeder restoration; it is highly efficient for identification of an optimal solution to restore all out-of-service loads with a given multi-feeder system topology. The solution is provided with a spanning tree structure that represents the final system topology, and a sequence of cyclic interchange operations that indicate necessary remedial switching actions transforming the initial post-fault system topology into the final system topology. The final system topology satisfies all the voltage, current and transformer capacity constraints. For a given multi-feeder system topology that satisfies all system constraints after the remedial actions are taken into account, the identified restoration plan that restores all out-of-service loads with a minimum number of switching actions is optimal.
- ✧ In collaboration with Pacific Northwest National Laboratory (PNNL), the proposed graph theoretic algorithm has been tested with a large scale test feeder model developed by PNNL and therefore its feasibility for practical applications is established. The proposed distribution restoration algorithm is implemented in the GridLAB-D environment. The simulation results demonstrate the potential to incorporate the proposed distribution restoration algorithm into a practical distribution automation system.

1.4 Dissertation Organization

The remaining of this dissertation is organized as follows: Chapter 2 provides a formulation of the concept of power system reconfiguration considering both real and reactive power balance as a multi-objective graph partitioning problem. Based on the multi-objective and multi-level graph partitioning techniques introduced in the same chapter, a graph-theoretic area partitioning scheme as well as a conceptual architecture for the proposed algorithm is developed. The important question of timing of the controlled system reconfiguration is also discussed. Numerical results obtained from a 200- and a 22,000- bus power system models are presented at the end of the chapter.

Chapter 3 describes the formulation of the distribution restoration problem as a multi-objective problem subject to a variety of constraints, and models the distribution restoration problem as a spanning tree search problem in graph theory. The optimality and complexity of proposed algorithm is also discussed. The GridLAB-D simulation environment and taxonomy feeder models that are used to validate the proposed algorithm are presented. At the end of this chapter, the simulation results using a 4-feeder 1053 node realistic distribution test system are provided.

Finally, the conclusions and suggestions for the future work are presented in Chapter 4.

CHAPTER 2. CONTROLLED POWER SYSTEM SEPARATION ON TRANSMISSION NETWORK

2.1 Introduction

System reconfiguration that intentionally partitions a power network into self-sufficient islands in anticipation of a degrading operating condition is an emergency control. It is designed to stop the propagation of disturbances, avoid uncontrolled system separation, and prevent wide area blackouts. This smart grid technique is an enhancement of the reliability and robustness of the power infrastructure. These islands are featured by minimized imbalance between generation and load. If the controlled system reconfiguration scheme is conducted appropriately, the impact of disturbances can be contained within the islands. Therefore, cascading events and further system separation within islands can be avoided. Furthermore, the overall efficiency of system restoration can be improved.

One of the important criteria to determine islanding boundaries by existing system reconfiguration methods is to minimize the real power generation and load imbalance within each island. This criterion is aimed at regulating the system frequency of each island within allowable limits. However, reactive power balance has not been incorporated in the development of power system reconfiguration algorithms. Reactive power plays an important role in supporting the voltage profile of a power system. Insufficient reactive power support leads to a low voltage profile that may result in voltage instability or undesirable line and generator tripping events. The reactive power deficiency in the Idaho area resulted in voltage instability that played a crucial role in the July 2, 1996, blackout [35]. A significant mismatch of the reactive power supply and demand causes high- or low-voltage conditions within islands. To keep the post-islanding system frequency and voltage profile within the acceptable limits, it is desirable to consider both real and reactive power balance in system reconfiguration techniques.

In this dissertation, a novel graph theoretic area partitioning algorithm is developed. This algorithm is able to partition a power network into k-disjoint areas while minimizing the real and reactive power generation load imbalance within each area. The proposed area partitioning algorithm is computationally efficient so that it is feasible to determine the optimal partition taking into account the vulnerable operating condition in a real-time environment.

The organization of remaining sections of Chapter 2 is as follows: Section 2.1.1 analyzes basic patterns of cascaded events leading to catastrophic. Section 2.1.2 surveys the industry practice of applying controlled system separation to prevent cascading failures. Section 2.2 formulates the concept of power system reconfiguration considering both real and reactive power balance as a multi-objective graph partitioning problem. Section 2.3 summarizes some basic concepts in graph theory, the multi-objective graph partitioning and the multilevel graph partitioning techniques. Section 2.4 introduces the proposed graph theoretic area partitioning scheme as well as a conceptual architecture for the proposed algorithm. The important question of timing of the controlled power system reconfiguration is discussed. Section 2.5 provides the simulation results using a 200-bus and a 22,000-bus power system models. Section 2.6 includes the conclusions.

2.1.1 Patterns of Cascaded Events in Blackouts

In general, the sequences of events in the major blackouts followed a common process. Typically, the cascaded events were initiated by a single event or multiple events, such as the 500-kV line outage (U.S. 1996), the generator tripping and the 345-kV line outage (U.S. and Canada 2003 [36]), the line outage (Italy 2003) and the coupling operation of busbars at a substation (Europe 2006).

Following the initiating events, the cascaded events took place sequentially. One component failure may trigger another event, which can bring successive line tripping and/or generator tripping. These subsequent events lead to power flow rerouting, overloads, voltage instability, and angle instability, which further weaken the system. As the cascaded events proceed, angle instability, power oscillations, and significant imbalances between the power supply and demand may take place, leading to a widespread voltage collapse and uncontrolled system splitting.

An excessive imbalance between load and generation after system splitting further caused a severe frequency drop [37] and ultimately led to a large-scale outage [38]. During the early stage of cascaded events, the cascading process can proceed at a relatively slow speed [10], such as in the U.S. and Canada 2003 blackout [36]. However, once a critical point is reached, the successive load and generator tripping events can spread promptly and uncontrollably [39]. At this point, a large-scale blackout is inevitable.

A weakened system condition is a contributing factor to four major blackouts shown in Table 1. When the system is highly stressed, power flows are high, the system voltage may decline and the power network components are highly loaded. As a result, the interactions between component failures tend to be stronger, and a single event is more likely to trigger other subsequent events that lead to a large blackout [40]. A summer peak-load profile, heavily loaded transmission lines, out-of-service transmission facilities due to the scheduled maintenance can further weaken the system.

Table 1. Major Blackouts in North America and Europe

Date	Location	Scale in terms of GW and Population	Collapse Time
Aug.10th, 1996	US-Western Interconnection	30.5 GW, 7.5M people	> 6 minutes
Aug.14th, 2003	Northeast US & Eastern Canada	62 GW, 50M people	> 1 hour
Sep. 28th, 2003	Italy	27GW, 57M people	> 25 minutes
Nov. 4th, 2006	Europe	17GW, 15M people	> 20 seconds

There are many causes of cascaded events that contribute to catastrophic outages. They typically include faults, undesired relay operations (including hidden failures), equipment failures or malfunctions, communication and information failures, and operational errors. Due to the mixture of the causes, prediction of the exact sequence of cascaded events that will take place is practically impossible. However, it is important to look into the fundamental patterns of cascaded events, i.e., which event can trigger other events. Some examples of fundamental patterns of cascaded events are shown as follows,

1) *Line Tripping Due to Overloading*. One important cause of cascaded events is the inappropriate relay operation. A study by the North American Electric Reliability Corporation (NERC) shows that protective relays are involved in about 75% of all major disturbances [41]. In major outage scenarios, a line fault can cause power flows to be rerouted, leading to the overload of other lines. As a result, the overloaded lines may be tripped due to a depressed voltage and/or high current, resulting in a low apparent impedance seen by an impedance relay. A good example is the undesirable zone 3 relay operation that does not involve a fault. The critical event for the 2003 U.S. and Canada blackout was an

inappropriate zone 3 relay operation caused by high real and reactive load currents and depressed voltages [36]. In the 2006 Europe blackout, several lines in the UCTE area were tripped by distance relays due to overloading.

2) *Undesirable Generator Tripping Caused by Over-excitation*. Line outages may cause low voltages and high reactive power demand on generators nearby, leading to tripping of these generator units by over-excitation protection equipment. The loss of generator units can reduce the reactive power supply in the system and cause further depression of the system voltage profile. As a result, cascading generator tripping events may be triggered by the operation of the over-excitation protection equipment. In the 1996 U.S. blackout, 13 generator units at the McNary plant were tripped by over-excitation protection equipment, which directly contributed to the final collapse. Another example is the 2003 U.S. and Canada blackout; 29 generators were tripped by over-excitation protection equipment, which triggered the first major power swing. These trips were caused by the generators' protective relays that responded to overloaded transmission lines and many of these trips were reported as under-voltage and over-current [36].

3) *Line Tripping due to Loss of Synchronism*. System disturbances, such as faults, line outages, generators tripping, and loss of load, can cause oscillations in machine rotor angles and system bus voltages, leading to a power flow swing. A line outage caused by an undesirable distance relay operation during a power swing and out-of-step condition is also a basic pattern. When the angle difference between two buses is sufficiently large due to a power swing, the impedance locus seen by the relay may enter the operating zone and trigger the line tripping. Distance relays operated under a power swing condition in the 2003 U.S. and Canada blackout, which further stressed the system [36]. In 2006 Europe blackout,

several lines were tripped by distance relays due to a loss of synchronism, such as the 380 kV lines Etzersdorf-Ernsthofen [38].

4) *Generator Tripping Due to Abnormal Voltage and Frequency System Condition*. As the cascaded events evolve, a loss of generation and load will affect the system voltage and frequency. Sustained low voltages may cause damage to the auxiliary system of the generators. Typically, generator under-voltage relays are set to trip at 0.9 p.u. of the normal operating voltage for turbine protection [**Error! Bookmark not defined.**]. In the 2003 U.S. nd Canada blackout and 1996 U.S. blackout, several generator tripping events were triggered by generator under-voltage relay operations [10,39]. High voltage in some area of the system can also contribute to generator tripping. In the 1996 U.S. blackout, five generators were tripped by a loss of field relay due to the high voltage [35]. Another pattern for the generator tripping events is the low/high system frequency. In the 1996 U.S. blackout, 31 generators were tripped by under-frequency relays to prevent the generators damage [35]. In the 2006 Europe blackout, several generator units were tripped due to under-frequency in the Western area and over-frequency in the North-Eastern area of the UCTE system [38].

5) *Under-frequency/voltage Load Shedding*. Automatic under-frequency load shedding (UFLS) scheme and under-voltage load shedding (UVLS) scheme may be triggered when the system voltage or frequency in some area falls below a pre-specified value. UVLS is designed to shed load to prevent a local area voltage collapse, and UFLS is aimed to rebalance load and generation within an electrical island once it is formed by a system disturbance [39]. The automatic load shedding scheme is operated by protective relays. In the 2003 U.S. and Canada blackout, about 25 000MW load was shed by UFLS [36]. In the 2003 Italy blackout, about 7000MW load was shed by the automatic load shedding Scheme [36].

2.1.2 Prevention of Cascading Failures by Controlled System Separation

After the initiating contingency, cascaded events may occur one by one. Further contingencies may weaken the operating condition and the system may lose synchronism and be separated into several islands. Those islands are usually accompanied by severe imbalance of the generation and load. If the generation and load within the island cannot be balanced properly, the system frequency may violate constraints and lead to further line and generator tripping events. Disintegration of the islands may evolve and finally blackouts occur.

Unlike the islands formed by uncontrolled separation, the islands determined by the proposed power system reconfiguration concept can minimize the imbalance between generation and load. Therefore, the system frequency within the island can be regulated within allowable limits and the islands formed by controlled separation are less prone to a system collapse. If the power system reconfiguration scheme is conducted appropriately, the cascading events and large scale blackouts can be avoided.

Controlled system reconfiguration can be performed by simultaneously tripping multiple lines on a partitioning boundary and is usually performed with Special Protection Schemes (SPSs). A survey covering 111 Special Protection Schemes (SPSs) in 17 countries shows that 6.3 percent of the surveyed SPSs are controlled system islanding schemes [42]. In the traditional system reconfiguration adopted by industry, the system separation boundaries are predefined according to off-line study and may not reflect the real-time system operating conditions and contingencies.

2.2 Problem Formulation

An objective of existing partitioning algorithms is to identify optimal cut sets of the sub-networks which minimize real power flows on the islanding boundary. A lower level of real power flows on the partitioning boundary lines indicates a good balance of MW generation and load, and lower MW interdependency between islands. However, a balance of real power does not imply that reactive power is also balanced. A small amount of MW power flow on the islanding boundary may be accompanied by a large MVar flow. Tripping of transmission lines that carry large reactive power flows can lead to insufficient reactive power support in one island. If the reactive power supply in MVar insufficient area is not increased in time, bus voltages may drop significantly and generators may become overloaded by an excessive demand for reactive power. As a consequence, reactive power demands may eventually exceed the sustainable capacity of MVar resources, leading to a voltage collapse.

A balanced reactive power supply and demand in each island helps to improve the voltage profile and enhance the ability of an island to withstand a disturbance. It is desirable to find a system reconfiguration plan that keeps the MW balance and also avoids insufficient MVar support caused by tripping of transmission lines on the islanding boundary that carry significant reactive power flows.

Graph theoretic islanding approaches have been proposed [7, 13, 18]. In these methods, a power network is converted into a weighted graph with buses and lines represented as vertices and edges, respectively. The absolute value of the MW flow on the line is used as the edge weight. Graph partitioning techniques are applied to divide a weighted graph into several smaller graphs with evenly distributed weights and minimized edge cut sets. A logical extension to existing graph partitioning methods is to assign two distinct weights to each edge, one for MW flow and the other for MVar flow. Consequently, the graph partitioning problem becomes the one of partitioning a graph into several disjoint sub-networks such that the edge cut sets with respect to different edge weight are minimized. At the same time, each sub-network has a roughly equal amount of vertex weights.

2.3 Graph Theory Foundation

2.3.1 Basic Concepts in Graph Theory

The basic concepts of Graph and Cut in graph partitioning are defined as follows.

Definition 2-1 (**Graph**)

A graph *G* is a pair (*V*, *E*) where *V* is a finite set and *E* is a set of 2-element subsets of *V* . Elements of *V* are called vertices and elements of *E* are called edges. *V* is the vertex set of *G* and *E* is the edge set.

An Undirected Graph *G(V,E)* is a graph in which edges have no orientations.

Definition 2-2 (**Cut**)

In graph theory, a cut is a partition of the vertices of a graph *G* into two disjoint subsets. The cut-set of the cut is the set of edges whose end points are in different subsets of the partition. In a weighted graph, the size of the cut is defined by the sum of the weights of the edges crossing the cut. A cut is *minimum* if the size of the cut is not larger than the size of any other cut.

2.3.2 Multi-objective Graph Partitioning

A traditional graph partitioning algorithm is only able to find the optimal partition with a single objective. However, in many engineering applications, there is a need to produce a partitioning with multiple optimization objectives. One example is the minimization of the number of wires cut by the partitioning as well as the propagation delay between chips in the VLSI domain. These problems can be formulated as a graph partitioning problem in which every edge is assigned multiple weights, and partitioning objectives are minimizing the edge-cut with respect to each of the multiple weights.

A multi-objective optimization is challenging since an optimal solution for one objective is not necessarily optimal for another. In the multi-objective partitioning problem, different edge weights increase the difficulty in finding the optimal solution. The simple combination-based approach, such as adding two weights to a single weight, is not always appropriate. In [43], an algorithm is proposed that can handle both similar as well as dissimilar edge weights, allowing tradeoff among different objectives and resulting in predictable partitioning. This algorithm combines multiple objectives into a single objective and applies a single objective algorithm to conduct partitioning. The way to combine multiple objectives is based on the intuitive notion of what constitutes a good multi-objective partitioning. A partitioning solution close to each optimal partitioning with respect to the single objective is considered to be good. The basic procedure to conduct a two-objective partitioning is shown below,

1) A single objective graph partitioning for the first objective is conducted. The best edge-cuts C_1 is obtained.

2) A single objective graph partitioning for the second objective is conducted. The best edge-cuts C_2 is obtained.

3) A combined weight for each line is obtained by the sum of the normalized edge weight with best edge-cuts C_1 and C_2 and weighted by the adjustable preference factor p, where w_1 and w_2 are different weights of each edge. The preference factor p is a number between 0 and 1.

$$w_{combined} = \frac{w_1}{c_1}p + \frac{w_2}{c_2}(1-p) \quad (2\text{-}1)$$

The distance that each edge-cut is allowed to vary from the optimal solution is controlled by the factor p. Thus, the preference factor p controls the tradeoffs among different objectives. Since all edge weights are normalized with a corresponding objective, they represent a fraction of the optimal cut set and can be combined [43].

4) A single objective graph partitioning is applied with the new combined normalized edge weights.

2.3.3 Multi-level Graph Partitioning

Graph partitioning with Minimum Ratio Cut is known to be NP-complete and has many applications in science and engineering. Graph partitioning algorithms have been developed. However, some of them are computationally expensive for large graphs. The multilevel graph partitioning scheme [44] is a state-of-the-art technique that significantly reduces the computation time while generating high quality partitions. The multilevel partitioning scheme does not partition the original graph directly. Rather, it first reduces the size of graph through a number of levels by collapsing vertices and edges. Then, the condensed graph is partitioned. Finally, a procedure is used to propagate and refine the solution through successive levels to the original graph.

Consider a weighted graph $G_0 = (V_0, E_0)$. The three stages of a multilevel partitioning scheme, as shown in Figure 1, are summarized here.

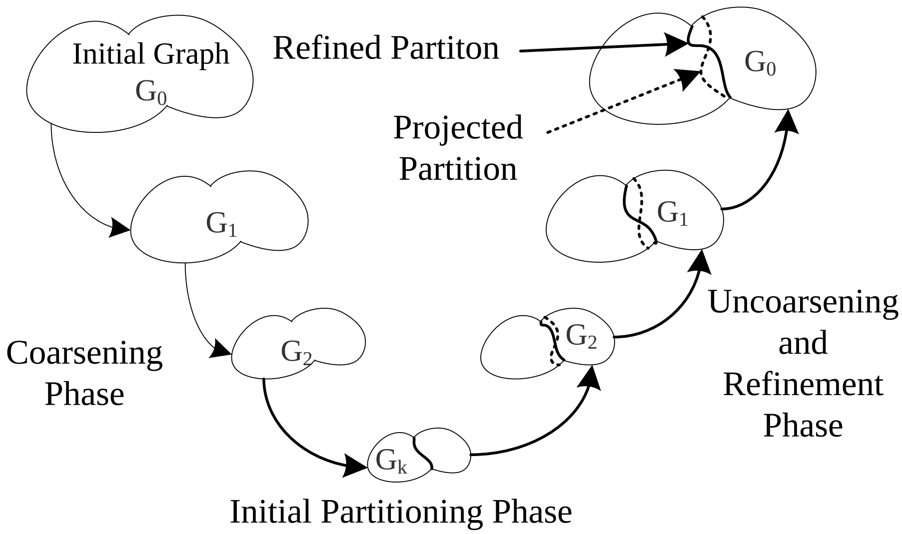

Figure 1. Multilevel Graph Partitioning

1) *Coarsening Phase*: The initial graph G_0 is transformed into a sequence of smaller graphs $G_1, G_2 \ldots G_k$ such that $|V_0| > |V_1| > |V_2| > \ldots > |V_k|$. A simple way to obtain the coarse graph is to group vertices of the graph into disjoint clusters and collapse vertices of each cluster into a single vertex.

2) *Partitioning Phase*: A partition P_k of the coarsest graph $G_k = (V_k, E_k)$ that minimizes the edge cut and satisfies the balancing constraints is computed. Since the size of coarsest graph G_k is small, various partition algorithms, e.g., recursive bisection, can be used to obtain the partition P_k.

3) *Uncoarsening and Refinement Phase***:** The partition P_k of the graph G_k is successively projected back to the original graph G_0 through intermediate graphs G_{k-1}, G_{k-2}… G_1, G_0. At each step of the uncoarsening phase, the partition is further refined to reduce the cut sets and improve the solution.

2.4 Proposed Power System Reconfiguration Scheme

2.4.1 Area Partitioning Algorithm

Based on the multilevel graph partitioning discussed in the previous section, an efficient power network area partitioning algorithm is developed [45]. The algorithm reported in [45] does not involve a graph simplification step for a large scale power network. Such a simplification step may lead to a loss of useful information, reducing the accuracy of partitioning. A coarsening and uncoarsening process is included in the multilevel graph partitioning algorithm that will be applied.

The network is modeled as an edge-weighted graph. Each bus of the power network is a vertex of the graph, each transmission line is an edge. The weights of an edge are absolute values of the MW and MVar power flows on the line, respectively. The graph of the power network is constructed off-line. The final graph is updated with information of topological changes and weights for the edges.

With the updated weighted graph, a multilevel recursive bisection algorithm is used to partition the weighted graph into several isolated areas. In this stage, a circuit partitioning tool, pMETIS that implements a multilevel recursive bisection algorithm is utilized [44]. pMETIS is a graph partitioning tool that has been widely used in VLSI design and its performance in terms of the cut size and computational time is excellent. As an example, it is capable of partitioning a graph with 15,606 vertices and 45,878 edges into 256 subareas with minimum cut set in 3.13 second on a PC [44]. With the fast computational speed, the proposed area partitioning algorithm has the potential to compute the system islanding configuration in a real time environment.

The optimal number of isolated areas, *k*, can be selected from several area partitioning scenarios ranging from two isolated areas to k_{max} areas, where k_{max} is the largest acceptable number of isolated areas for the specific system. The optimal *k* area partitioning is the one with minimum loss of load among all acceptable partitions.

2.4.2 A Framework of Proposed System Reconfiguration Strategy

The power network is converted to an edge-weighted graph before graph partitioning is initiated, according to the real-time power flow solution. Each bus of the power network is a node or vertex of the graph G. Each transmission line of the one-line power system diagram is an edge of graph G. The weights w_1^i and w_2^i of each edge *i* of graph G are assigned according to the absolute values of MW and MVar power flow of the corresponding transmission line, respectively, i.e.,

$$w_1^i = \Sigma|P^i| \quad (2\text{-}2)$$

$$w_2^i = \Sigma|Q^i| \quad (2\text{-}3)$$

As a result, the best edge-cuts C_1 and C_2 in equation (2-1) are calculated by

$$C_1 = min \sum_{i \in B} w_1^i \quad (2\text{-}4)$$

$$C_2 = min \sum_{i \in B} w_2^i \quad (2\text{-}5)$$

where, *B* in equations (2-4) and (2-5) is an edge set that includes all the edges on the area partitioning boundary.

Since real and reactive power balance within the island must be achieved, a two stage system reconfiguration strategy is proposed. There are two constraints for the subsystem formed by system reconfiguration:

1) *Real Power Balance Constraint (RPBC)*: In each island, MW generation is equal to or larger than MW load.

2) *Boundary Bus Voltage Constraint (BBVC):* Voltages at the buses on the islanding boundary lines after system reconfiguration should be maintained within tolerances by industry practice (0.95 pu to 1.05 pu for instance). A flow chart of the proposed strategy is given in Figure 2.

At Stage One, the area partitioning algorithm only considers minimization of MW flow on the islanding boundary. Based on the partitioning solution, if RPBC is not satisfied, or if MW load is higher than MW generation in one island, the amount of load to shed is determined and the optimal islanding strategy is the solution obtained by Stage One area partitioning. If RPBC is satisfied, then BBVC is checked. If low bus voltages on the islanding boundary are expected after islanding, then go to Stage Two partitioning.

At Stage Two area partitioning, a multi-objective multilevel graph algorithm is applied. The detailed procedure is as follows:

1) A single objective graph partitioning is computed with the edge weight equal to the absolute value of MVar flow on the transmission line, and the best edge-cuts C_q for this objective is recorded.

2) A single objective graph partitioning is computed with the edge weight equal to the combined weight $w_{combined}$, where $w_{combined}$ can be obtained from equation (2-1) with the best edge-cuts C_p obtained at Stage One partitioning, the best edge-cuts C_q obtained at the last

step and the preference factor *p*. The preference factor *p* is initiated to reduce the MVar flow on the islanding boundary. The choice of *p* depends on the specific system structure and operating conditions.

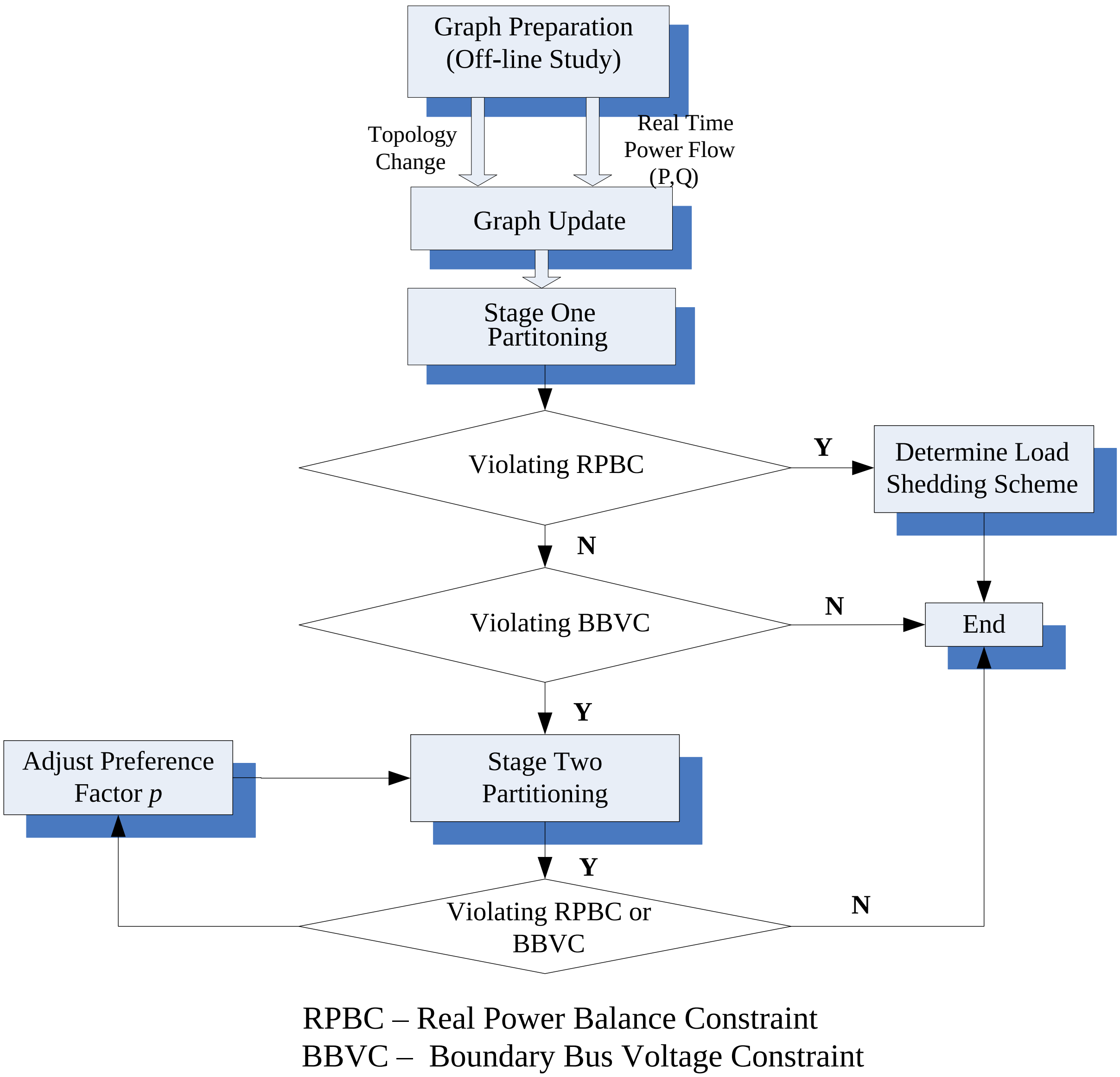

Figure 2. Proposed Area Partitioning Procedure

3) A single objective graph partitioning is applied with the new combined normalized edge weights.

After Stage Two partitioning, RPBC and BBVC are checked again. If both constraints are satisfied, this partitioning solution is chosen as the optimal solution. Otherwise, modify the preference factor *p* and apply Stage Two area partitioning again. The multi-objective graph partitioning algorithm is able to enhance the minimization of real power flow and reduce the ability to minimize reactive power flow on the islanding boundary by increasing the preference factor *p*. In contrast, decreasing the value of *p* would reduce the total MW flow on the islanding boundary and increase the total MVar flow on the boundary.

2.4.3 Timing of the Intentional Power System Reconfiguration

The controlled system partitioning, as a "last resort" measure to prevent cascading events, is triggered when the system is in an extremis crisis [46]. Several fundamental patterns of cascaded events are summarized in [47].These subsequent cascaded events may lead to widespread outages, uncontrolled system splitting, and the system collapse due to overloads, voltage and angle instability.

Real time vulnerability assessment that recognizes patterns of cascaded events and predicts an instability condition is an effective way to determine the timing of controlled self-healing reconfiguration. When vulnerability analysis indicates that the system is threatened by a cascading sequence of events, the controlled system partitioning can be initiated. In [48], the initiating time for controlled islanding is determined by predicting impending loss of synchronism and cascading events with decision trees (DTs).

A Phasor Measurement Unit (PMU) based on-line monitoring scheme that identifies the pattern of loss of synchronism is proposed in [4]. This method is computationally efficient, which makes it possible for fast remedial controls to mitigate system instability and prevent an uncontrolled system separation. In this method, the Maximal Lyapunov Exponent (MLE) of the power swing after the disturbance is calculated with real-time PMU data. If the MLE of the corresponding power swing is negative, this power swing is asymptotically stable; otherwise, it is considered unstable [4]. This result is used to evaluate whether or not an electromechanical swing will lead to an out-of-step condition. Once an unstable power swing is captured and rotor angle instability is predicted by the above method, self-healing reconfiguration is initiated.

2.4.4 Special Protection Scheme Architecture

Fast line tripping actions are required to preserve the stability of generators and avoid equipment damage [49]. An advanced wide-area stability and control system (WACS) [50] enables real-time control and protection. The controlled islanding actions can be initiated by a special protection system (SPS). A conceptual relaying system for controlled islanding is illustrated in Figure 3.

This system consists of one central control unit (CCU) and several substation control units (SCUs). CCU acquires system data such as topology and power flows from SCUs and generates the system separation strategy using the proposed area partitioning algorithm. Power flow data can be obtained from on-line Energy Management Systems (EMSs). SCUs receive the system separation command from CCU and send breaker opening signals to specific auxiliary relays. These relays then send tripping signals to the appropriate circuit breakers. To ensure reliable and fast information transfer between CCU and SCUs, a dedicated communication network, such as a synchronous optical network (SONET), would be needed.

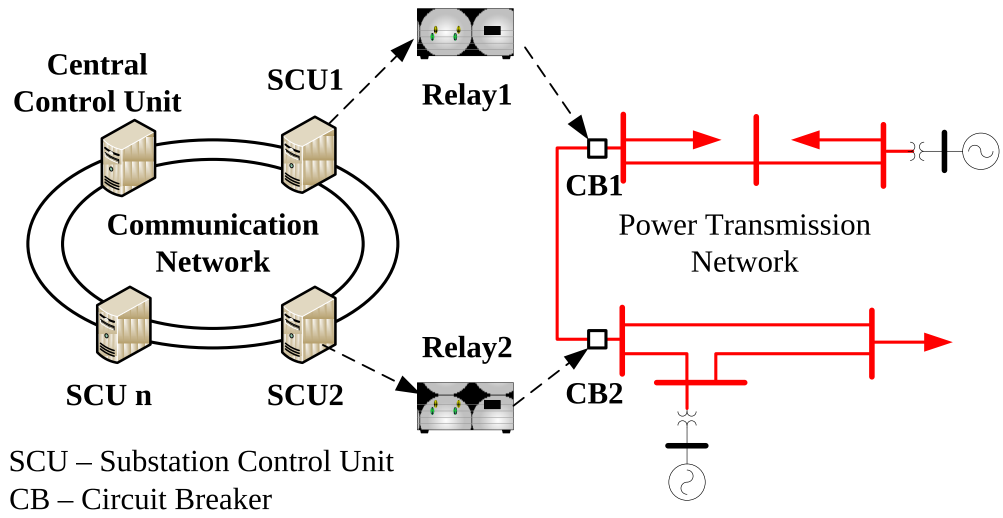

Figure 3. A Conceptual Relaying Architecture for Controlled System Separation

2.5 Numerical Results

2.5.1 Simulation with a 200-Bus System

A 200-bus system that is a variation of the simplified model of the Western Interconnection in North America is used to evaluate the performance of the proposed network partitioning algorithm. The one-line diagram is shown in Figure 4.

This system is operating under a peak load condition with a total generation of 64,417.32 MW, 17,236.9 MVar, and a total load of 63,510.41MW and 16,171.75 MVar. The simulation is based on PSS/E power flow and time-domain simulation results. A cascading scenario is created on the 200-bus system, and the sequence of events is as follows,

1) At t=0 seconds, three transmission lines (196-197, 76-181, 69-76) are out-of-service.

2) At t=60 seconds, line 72-197 is de-energized due to a line fault.

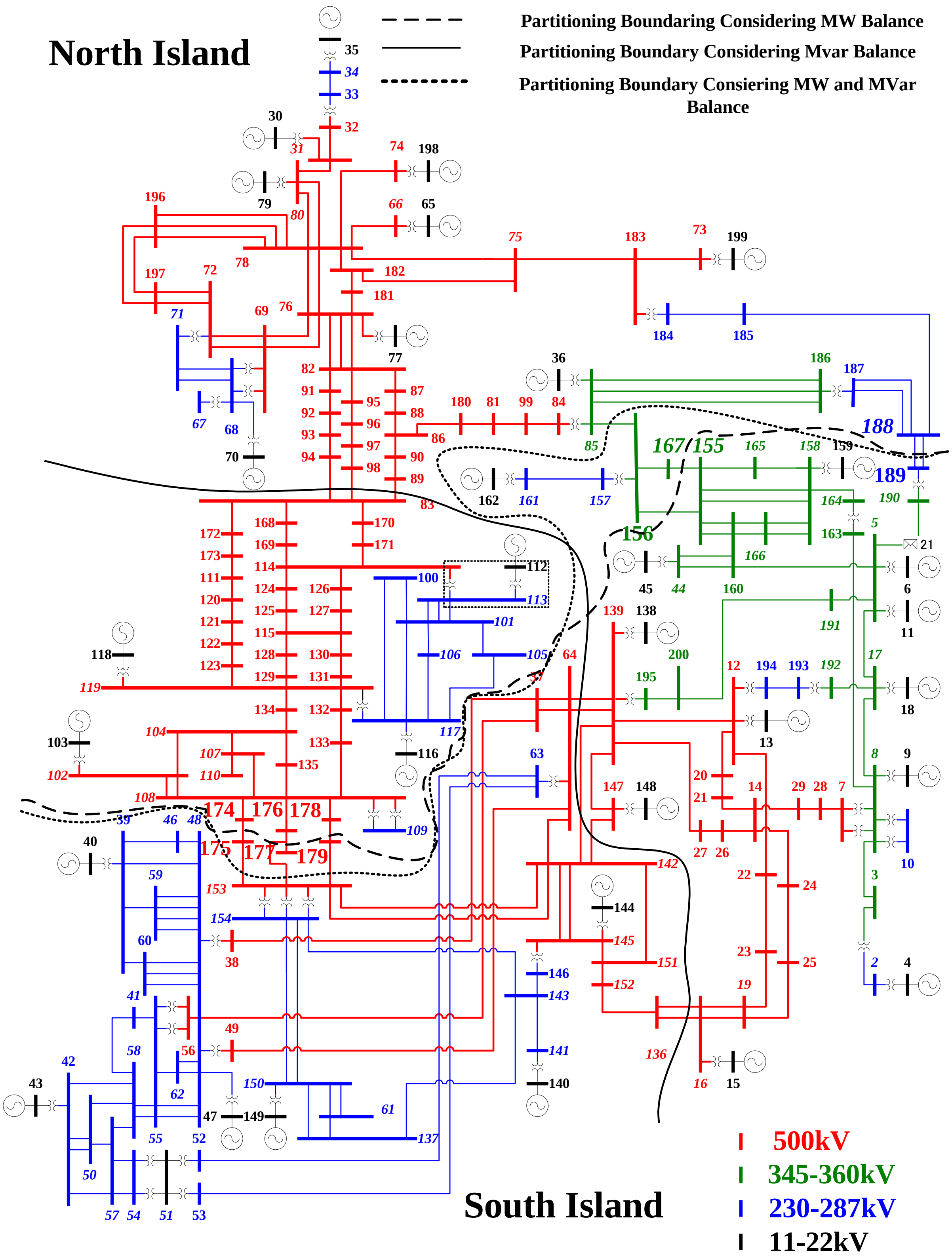

Figure 4. 200-Bus System

3) At t=120 seconds, line 78-196 is de-energized due to a line fault. Generator G70 at bus 70 becomes overloaded.

4) At t=240 seconds, generator G70 hit its field thermal limit and is tripped by over-excitation protection.

In this cascading scenario, successive tripping of the lines leads to power flow rerouting and overloads. After tripping of generator G70, power swings become lightly damped. Progressive drops in bus voltage are observed with rotor angle instability. The generator angle difference between generator G77 in North Island and generator G15 in South Island, observed in Figure 5, increases continuously after t=240 seconds and finally exceeds 180° at t=263 seconds. As shown in Figure 6, the voltage collapse occurs at about 280 second. Since the voltage dependant load characteristics are considered in the dynamic model, with the cascading events, the total load in the system is reduced to 61,039.34 MW and 15,227.48 MVar at t=240 second.

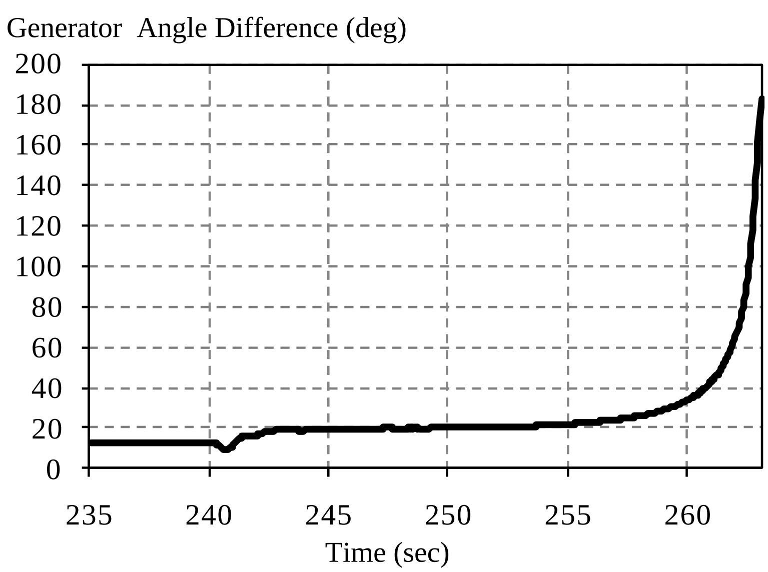

Figure 5. Generator Angle Difference without Islanding Strategy

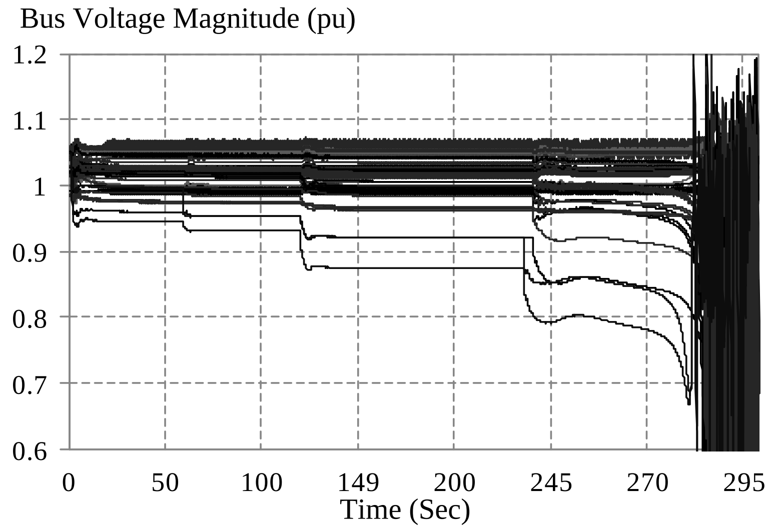

Figure 6. Bus Voltages without Islanding Strategy

The PMU and MLE based angle stability monitoring technique mentioned in Section 2.4.3 is applied to determine the timing to trigger the controlled partitioning. The calculated MLE value for the power swing initiated at t=240 seconds, following the generator tripping event, is 11.6148, which indicates this power swing is unstable and it can lead to an out-of-step condition. Therefore, system partitioning is initiated at 1 second after tripping of generator G70. This scenario is verified with the time domain simulation result.

1) *System Reconfiguration Performance without Considering Reactive Power Balance*: In order to prevent cascading events, the system is separated into two areas, i.e., North Island and South Island, using the proposed area partitioning algorithm. The performance of system reconfiguration without considering reactive power balance is evaluated first. Only MW flow on the partitioning boundary lines is minimized.

The edge cut sets and corresponding absolute values of real and reactive power flows on the islanding boundary are shown in Table 2. The Stage One partitioning boundary that has minimized total MW flow on the boundary lines is given in Figure 4. Note that the system is partitioned into two islands, North Island and South Island, with a roughly equal size. The total real power flow across the islanding boundary is 893.5 MW. The total real power load and generation in North Island are 37203.4 MW and 37607.2 MW, respectively. The total real power load and generation in South Island are 23835.9 MW and 24335.5 MW, respectively. Both islands contain significant generation resources and satisfy the Real Power Balance Constraint (RPBC). As shown in Figure 7, after controlled system partitioning, South Island is successfully stabilized and all bus voltages are higher than 0.95 pu.

Table 2. Stage One Partitioning Cut Set

Cut Set	174-175	176-177	178-179	156-155	155-167	189-188(1)	189-188(2)	Total
MW	239.2	240.4	255.0	80.0	45.6	17.5	15.8	893.5
Mvar	402.8	405.9	430.8	30.0	41.6	13.9	8.3	1333.3
There are two transmission lines between bus 188 and 189.								

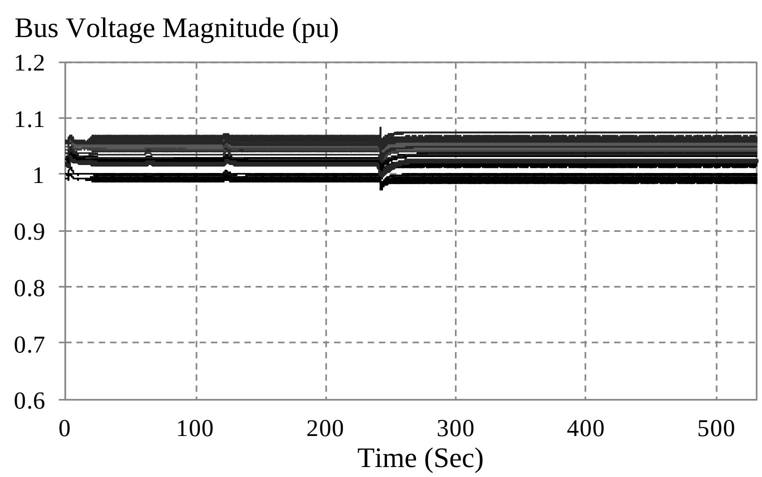

Figure 7. South Island Bus Voltages

Stage One partitioning does not consider the objective of minimizing the total MVar flow on partitioning boundary lines. As shown in Table 2, three transmission lines that carry about 1239.5 MVar flow in total are on the islanding boundary. The direction of the MVar flow on these three transmission lines is from South to North, which is the opposite direction of the MW flow. Tripping of these lines that carry a large amount of MVar flow will cause insufficient reactive power support in the area adjacent to the islanding boundary in North Island. As a result, after tripping of lines on the islanding boundary that separates the system into two islands. Significant voltage drop occurs at a few buses in North Island. The bus voltages that are lower than the 0.95 pu limit in North Island are listed in Table 3.

Table 3. Low Bus Voltages in North Island

Bus	104	107	108	111	174	176	178	196
Voltage(pu)	0.934	0.914	0.916	0.908	0.916	0.916	0.916	0.904

In Table 3, bus voltages at eight buses are below 0.95 pu. Although bus 196 is far from the partitioning boundary, two 500 kV lines connected with this bus are de-energized in the cascading process that leads to the low voltage profile at this bus. If a reactive power device such as a shunt capacitor is switched on, the low voltage at this bus can be avoided.

Except for bus 196, all other seven buses are close to buses 174, 176 and 178 that are on the system partitioning boundary. The low bus voltages in the adjacent area of the islanding boundary in North Island cause overloading of the generator at Bus 103. The plot in Figure 8 shows that the generator field voltage (EFD) at bus 103 is increased to 1.15 pu after the system reconfiguration. At t=350 seconds, the generator bus 103 is tripped by over-excitation protection. This is due to the fact that the generator field voltage at bus 103 continuously exceeds threshold pick-up value of the generator field voltage capability limit for 100 seconds [51]. As soon as the generator at bus 103 is tripped, a voltage collapse occurs at North Island. Figure 9 shows bus voltages at North Island during the cascading events and system reconfiguration.

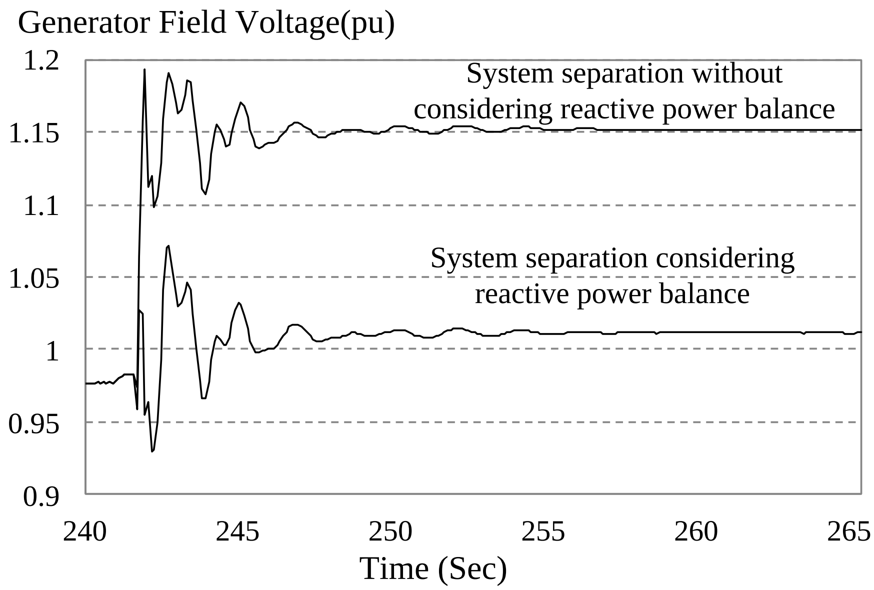

Figure 8. Generator Field Voltage at Bus 103

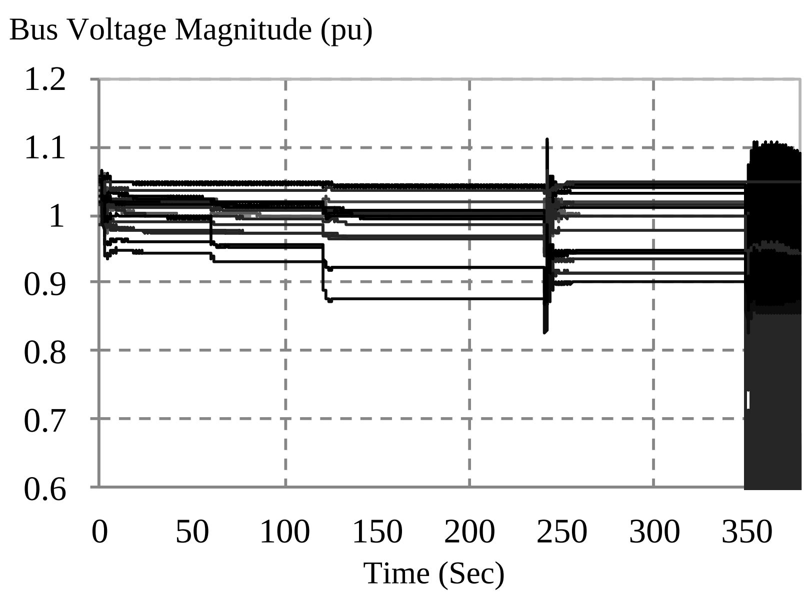

Figure 9. North Island Bus Voltages

In this simulation case, the system reconfiguration strategy without considering reactive power balance successfully prevents a voltage collapse at South Island that has abundant reactive power support but fails to stabilize North Island.

2) *System Reconfiguration Performance Considering Reactive Power Balance*: Since there is insufficient reactive power support and a low voltage profile exists in the boundary area of North Island after the system reconfiguration based on Stage One partitioning, Stage Two area partitioning described in Section 2.4.2 is conducted. The area partitioning boundary with the objective of minimizing MVar flow on the islanding boundary is shown in Fig. 4. The islanding boundary obtained with this objective divides the system into East Island and West Island, which is significantly different from the islanding boundary obtained at Stage One. The total minimized MVar flow on the islanding boundary is 490.3 MVar. Note that it is much smaller than MVar flow on the islanding boundary without considering reactive balance.

The new combined edge weight is calculated with equation (2-1), where c_1 = c_p=893.5 and c_2 = c_q=490.3. The preference factor is selected as 0.7. The calculated system partitioning boundary with new combined edge weights is shown in Figure 4. This boundary is close to the one obtained at Stage One partitioning geographically. However, the MVar flows on partitioning boundary lines are significantly reduced.

The edge cut set and corresponding absolute values of real and reactive power flows and new combined edge weights are shown in Table 4. The total real power load and generation at North Island are 36513.4 MW and 37178.1MW, respectively. The total real power load and generation at South Island are 24525.9 MW and 24764.6 MW, respectively.

Both islands contain significant generation resources and satisfy the Real Power Balance Constraint (RPBC).

Table 4. Partitioning Cut Set Considering Real and Reactive Balance

Cut Set	175-153	177-153	179-153	85-156	189-188(1)	189-188(2)	Total
MW	239.2	240.4	255.0	326.6	17.5	15.8	1094.5
Mvar	188.0	191.8	237.6	78.0	13.9	8.3	717.6
Combined Weight	302.4	305.7	345.2	303.6	22.2	17.5	1296.5
There are two transmmision lines between bus 188 and 189							

After the system is partitioned according to the boundary shown in Table 4 at 1second after tripping of generator G70, both islands are stabilized. As shown in Figure 10, only the bus voltage at bus 196 in North Island is stabilized at 0.905 pu, which is lower than the 0.95 pu limit, all other voltages are equal to or higher than 0.95 pu. No generator exceeds their field capability limits. The Boundary Bus Voltage Constraint (BBVC) is satisfied. Figure 11 shows that the stable frequency of North Island and South Island is 60.05 Hz and 59.97 Hz, respectively.

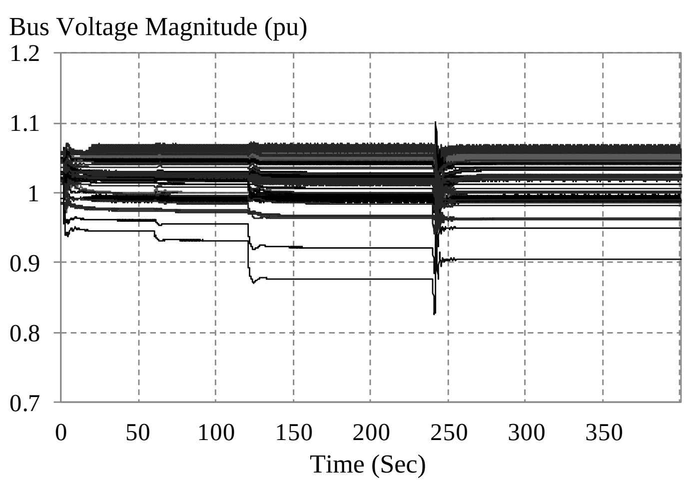

Figure 10. Bus Voltages with Reactive Power Balancing Islanding

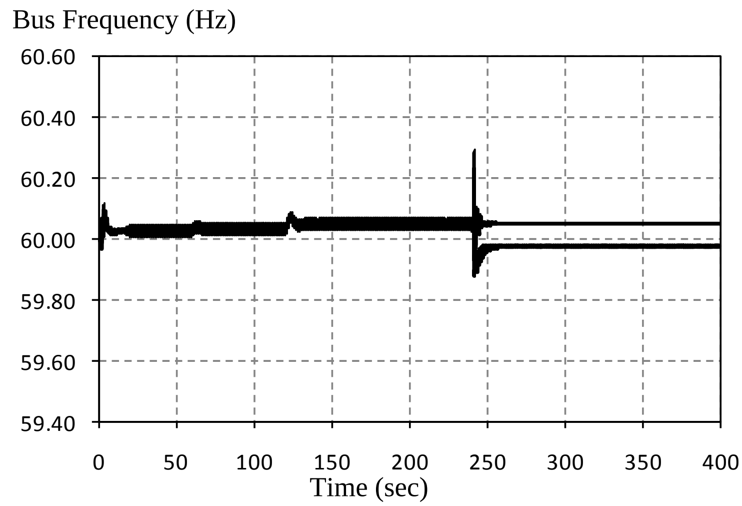

Figure 11. Bus Frequencies with Reactive Power Balancing Islanding

2.5.2 Simulation with a 22,000-Bus System

To evaluate the computational efficiency of the developed area partitioning algorithm, the algorithm is tested with a 22,000 bus system, representing Eastern Interconnection in North America. After converting this network into a weighted graph, 22,000 vertices and 32,749 edges are obtained. To partition this network into 2, 3, 4 islands with one single objective multilevel graph partitioning, the computation time based on a 2 GHz Pentium CPU with 1GB RAM is 0.07 seconds, 0.081 seconds and 0.09 seconds, respectively. Since the proposed multi-objective multilevel partitioning algorithm involves three single objective partitioning processes, the computation time for this 22,000 bus system with proposed MVar balance is less than 1 second. The computational performance of the proposed algorithm is expected to meet the requirement for a real time environment.

The simulation results based on the multi-level partitioning algorithm for a two-island case of the 22,000-bus system are given here.

1) Only Minimizing the Real Power Flow on the Islanding Boundary: The number of edge cuts is 299 for two islands. The total real and reactive power flow on the islanding boundary of two islands are 4708 MW and 2913.5 MVar, respectively. The maximum reactive power flow on one edge of the boundary is 202.4 MVar, the real power flow on this edge is 26.2 MW.

2) Only Minimizing the Reactive Power Flow on the Islanding Boundary: The number of edge cuts is 325 for two islands. The total real and reactive power flow on the islanding boundary of two islands is 6913.2 MW and 1434.7 MVar, respectively. The maximum reactive power flow on one edge of the boundary is 101.5 MVar while the real power flow on this edge is 135.8 MW.

3) Minimizing Both Real and Reactive Power Flows on the Islanding Boundary: The preference factor p is selected to be 0.7. The number of edge cuts is 308 for two islands. The total real and reactive power flow on the boundary of two islands is 5426.7 MW and 1734.7 MVar, respectively. The maximum reactive power flow on one edge of the boundary is 134.4 MVar and the real power flow on this edge is 208.7 MW.

Figure 12 and Figure 13 compare the actual and normalized values of total MW and MVar flow on partitioning boundary lines on the 22,000 bus system obtained by Step 1 or Step 2 partitioning (that only minimizes MW or MVar flow on the boundary lines) and those obtained by Step 3 partitioning (that minimizes both MW and MVar on the boundary lines). Note that the proposed multi-objective partitioning algorithm provides a good solution that minimizes both real and reactive power flows on the islanding boundary. The algorithm identifies a partitioning that represents a good tradeoff between the two objectives.

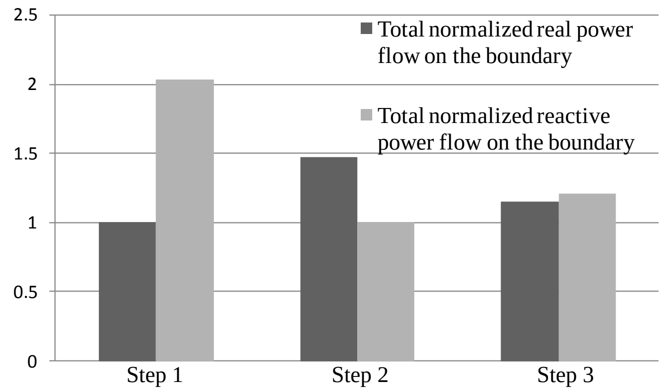

Figure 12. Normalized Edge-Cut Results with Different Partitioning Objectives

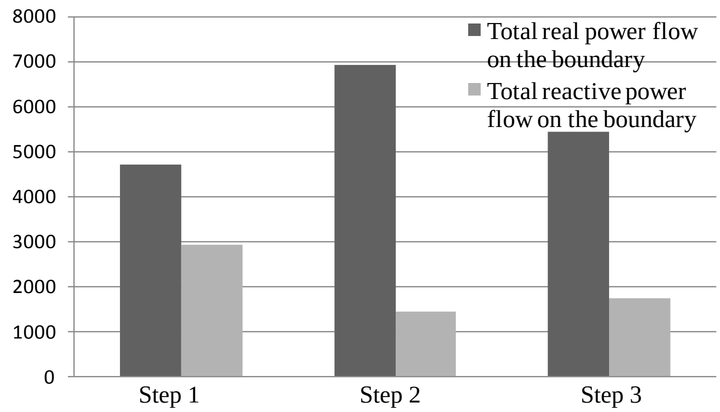

Figure 13. Edge-Cut Results with Different Partitioning Objectives

2.6 Summary

In response to disturbances, a self-healing system reconfiguration that splits a power network into self-sufficient islands can stop the propagation of disturbances and avoid cascading events. In this research work, an area partitioning algorithm that minimizes both real and reactive power imbalance between generation and load within islands is proposed. More balanced reactive power supply and demand in each island could avoid the low voltage profile after system separation caused by tripping transmission lines that carry large reactive power. The proposed algorithm is a smart grid technology that applies a highly efficient multilevel multi-objective graph partitioning technique. Thus, it is applicable to very large power grids. The proposed algorithm has been simulated on a 200- and a 22,000- bus test systems. The results indicate that the proposed algorithm improves the voltage profile of an island after the system reconfiguration compared with the algorithm that only considers real power balance. In doing so, the algorithm maintains the computational efficiency. The proposed area partitioning strategy has the capability to enhance the grid's shock absorption capability with respect to cascading failures.

CHAPTER 3. DISTRIBUTION SYSTEM RESTORATION

3.1 Introduction

Development of a self-healing power network that is able to anticipate and response to disturbances has been envisioned in [1] to enhance system reliability and customer satisfaction in the future power grid. Distribution restoration plays a critical role in the future “Smart Grid” to enable the power network at the distribution level a self-healing capability. Such a distribution restoration procedure refers to the process of changing open/closed states of tie switches and sectionalizing switches to restore loads that are disconnected from the grid due to fault isolation actions. The loads in the out-of-service area should be restored as quickly as possible after the fault is isolated. A restoration plan with minimized switching operations and an optimized switching sequence will reduce the impact of outages and enhance system reliability.

The distribution system restoration problem is a multi-objective, non-linear, combinatorial optimization problem with numerous constraints, including topology constraints, electrical and operating constraints. A large number of components in the distribution system and complicated generation and load models add to the complexity of a difficult problem.

A distribution network can be represented by a graph $G (V, E)$ that contains a set of vertices V and a set of edges E. Therefore, the distribution system restoration problem can be formulated as a problem of identifying the desired graph topology subject to various constraints. In this research, a graph theoretic search algorithm is proposed to identify a post-outage distribution system topology that will require a minimum number of switching operations. The proposed algorithm has the following features:

1) It not only finds the final system topology, but also provides a feasible switching operation sequence leading to the proposed final system topology.

2) A minimum number of switching actions is achieved given the distribution system topology after remedial actions that may be needed to remove constraint violations are taken into account. That is, if a system topology that can restore all out-of-service loads is found, the number of switching operations leading to such a system topology is minimum.

3) A three-phase unbalanced power flow model is developed that is used to determine whether a proposed solution satisfies the electrical and operating constraints.

4) The simulation time on a realistic distribution feeder model is in the order of seconds. Therefore, the proposed distribution system restoration strategy is promising as a decision support tool for distribution restoration planning and operation.

The organization of remaining sections of Chapter 3 is as follows: Section 3.2 describes the formulation of distribution restoration as a multi-objective problem subject to several constraints. Section 3.3 provides an explanation of basic concepts in graph theory and presents an algorithm to search for all spanning trees of a graph without duplication. Section 3.4 transforms the distribution restoration problem into one of the spanning tree search problem in graph theory, and proposes a graph theoretic distribution restoration algorithm. The optimality and complexity of the proposed algorithm is discussed. In Section 3.5, the GridLAB-D simulation environment is discussed together with taxonomy feeder models that are used to validate the proposed algorithm. Section 3.6 provides the simulation results using a 4-feeder 1053 node realistic distribution test system. Section 3.7 provides the conclusion of this chapter.

3.2 Problem Formulation

Distribution system restoration is intended to promptly restore as much load as possible in the areas where electricity service is disrupted following a fault. After the loads are restored, the final network topology should retain a radial structure, and satisfy all the electrical and operating constraints. The restoration process should be completed efficiently in order to reduce outage durations, thereby enhancing customer satisfaction. An efficient restoration plan should be established quickly to assist operators in the distribution operating center so that they can take remote control actions or dispatch maintenance crews to implement the restoration plan. Moreover, the restoration plan should provide not only a feasible system topology but also a sequence of switching operations to reach the final configuration.

The typical distribution system structures that are adopted by electric utilities include radial and loop systems. A radial system is characterized by having only one path connecting the power source and each customer. The radial system is the cheapest structure and most widely applied by the utilities. Over ninety-nine percent of the distribution systems in North America are radial [52]. A loop system has at least two paths that connect power sources and each customer. As a result, it is more reliable than a radial system due to an alternative power source to each customer. However, a loop system is generally more expensive than a radial system. The additional costs are needed for more conductors, higher conductor capacity, switching and protection devices. Moreover, the design of a protection scheme in the loop system requires proper coordination in either direction.

In this dissertation, the distribution system restoration through feeder reconfiguration is focused on the radial distribution system and formulated as a constrained multi-objective problem, i.e.,

Objectives:

Min n_{sw} (Minimizing the total number of switch operations)

Max $\sum_{i \epsilon N_{res}} S_i$ (Maximizing the amount of total load restored)

Subject to

i) $|I_l^{min}| \leq |I_l| \leq |I_l^{max}|, l \epsilon L_{en}$ (3-1)

ii) $|V_k^{min}| \leq |V_k| \leq |V_k^{max}|, k \epsilon B_{en}$ (3-2)

iii) $P_j^2 + Q_j^2 \leq (S_j^{maxT})^2, j \epsilon F$ (3-3)

iv) Radial network structure is maintained,

v) Unbalanced three-phase power flow equations are equality constraints.

Where,

n_{sw} is the number of switch operations required to achieve the final configuration,

N_{res} is the set of restored buses,

S_i is the total MVA power of the load at bus *i*,

I_l is the current flows through a distribution line *l*,

I_l^{min} , I_l^{max} are the lower and upper limit of the line current on distribution line *l*, respectively,

V_k is the bus voltage of bus k,

V_k^{min}, V_k^{max} are the lower and upper limit of the bus voltage at bus *k*, respectively,

L_{en} is the set of lines that are in service, B_{en} is the set of buses that are in service,

P_j is the MW power injected into feeder j, Q_j is the MVar power injected into feeder j,

S_j^{maxT} is the maximum transformer capacity at feeder j,

F is the set of all feeders.

The objectives of the algorithm include minimizing the total number of switching operations during the restoration process and maximizing the amount of load to be restored in the out-of-service area. Constraints (i) and (ii) show that the line current and bus voltage should be maintained within acceptable operating limits. Constraint (iii) shows that the total load of each feeder should not exceed the maximum capacity of the supplier transformer.

3.3 Graph Theory Foundation

3.3.1 Basic Concepts in Graph Theory

A few basic concepts related to the tree structure in graph theory are defined as follows:

Definition 3-1 (Path and Cycle)

A ***path*** in a graph is a sequence of vertices such that from each of its vertices there is an edge connecting to the next vertex in the sequence. A ***cycle*** is a path such that the starting vertex and ending vertex are identical.

Definition 3-2 (Connectivity)

In an undirected graph *G*, two vertices *u* and *v* are ***connected*** if *G* contains a *path* from *u* to *v*. A graph *G* is connected if every pair of distinct vertices in the graph is connected through some paths.

Definition 3-3 (Tree and Spanning Tree)

A ***tree*** *T* is a connected graph that contains no cycle. A ***spanning tree*** *T* of a connected, undirected graph *G* is a ***tree*** composed of all vertices and some or all the edges of G. An undirected graph *G (V, E)* is a graph in which edges have no orientations. An edge in a spanning tree *T* is a *branch* of T. An edge of *G* that is not contained in a spanning tree *T* of this graph *G* is called a *chord*.

Let *T* be a spanning tree with n vertices. The following statements are equivalent.

- *T* is connected and has no cycle.
- *T* has n vertices and n − 1 edges and has no cycle.
- *T* is connected and the removal of any edge disconnects *T*.
- Any two vertices of *T* are connected by exactly one path.
- T contains no cycle, but the addition of any new edge creates a cycle.

Definition 3-4 (Fundamental Cut Set)

In a connected graph *G*, a cutset is a set of edges whose removal would break *G* into two components [53]. Considering a spanning tree *T* in *G* and an edge *e* in *T*, a fundamental cutset $S_e(T)$ is a cutset which contains exactly one edge e in *T* and some other edges in $G-T$ that breaks *G* into two components if necessary, where $S_e(T)$ stands for a fundamental cutset of *e* with respect to *T*. The fundamental cutset $S_e(T)$ can be found by a depth-first-search on *T*.

Theorem 3-1 (A Characteristic of Spanning Tree[53])

With respect to any of its spanning trees, a connected graph *G* of *n* vertices and *e* edges has *n-1* tree branches and *e-n+1* chords.

3.3.2 Searching for All Spanning Trees without Duplication

In a graph *G*, an initial spanning tree *T* can be transformed into any other spanning tree *T'* through a single or multiple cyclic interchanges [53]. A typical cyclic interchange operation consists of adding an edge to the initial spanning tree that forms a cycle and deleting another edge in this cycle. However, a tree may be generated repeatedly in this process. A graph theoretic algorithm in [54] that generates spanning trees without duplication provides a systematic solution to the above problem. A few notions and definitions in graph theory that formalize the above algorithm are presented as follows,

Notions: $\oplus$ stands for "exclusive or" of two sets; $A-B$ stands for the set containing all the elements of *A* that are not in *B*.

Definition 3-5 (**Selective Cyclic Interchange Operation**): Starting from a tree T_0, some other trees can be obtainable by replacing an edge *e* of tree T_0 with another edge in the fundamental cutset $S_e(T_0)$, and the resulting trees are distinct. Such an operation can be represented in the following form, where *t* represents all trees that are transferred from T_0.

$$\{t|t = T_0 \oplus\{ee_i\}, e_i \in S_e(T_0), e_i \neq e\} \tag{3-4}$$

An example of cyclic interchange operation is shown in Figure 14. Some other trees can be generated by replacing edge *d* of tree T_0 with another edge in the fundamental cuset $S_d(T_0)$. Since the edges in the fundamental cuset $S_d(T_0)$ besides edge *d* are edge *c* and edge *h*, tree T_1 and tree T_2 can be obtained by replacing edge *d* with edge *c* and with edge *h*, respectively. Note that either edge *c* or edge *h* is a chord of the graph *G* with respect to tree T_0.

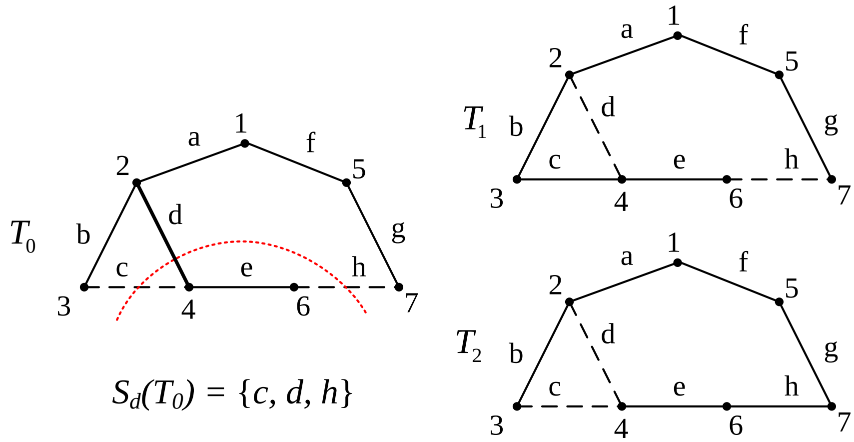

Figure 14. An Example of Cyclic Interchange Operation

An iterative procedure to generate all trees without duplication based on the definition (3-1, 3-4) is as follows,

1) A reference spanning tree T_0 is generated for graph G. The edges in G are ordered such that each subset of initial k edges is a connected graph, $k = 1, 2, \ldots, v$.

2) Each edge e_i of T_0 is replaced by an edge e_k in the fundamental cutset of e_i with respect to T_0 ($e_k \in S_{e_i}(T_0)$), to generate a class of spanning trees T_{e_i}, $i=1, 2, \ldots, v-1$.

3) Then starting from T_{e_i}, a class of spanning trees $T_{e_i e_j}$ are generated by replacing an edge e_j with an edge $e_k \in S_{e_j}(T_0) \cap S_{e_j}(T_{e_i})$, where $i<j\leq v-1$, where v is the number of vertices of graph G. Edges are replaced in an ascending order following the sequence provided at step 1).

4) Repeating the procedure at step 3), all spanning trees of graph G can be generated sequentially without duplication.

3.4 A Graph-Theoretic Distribution Restoration Strategy

3.4.1 Distribution Network Topology and Spanning Tree

A distribution network is formed by interconnected distribution feeders. The feeders are connected with each other through tie switches. If a load node is modeled as a vertex and a feeder line section is viewed as an edge in the graph, the distribution network can be represented as a connected graph *G*. The radial structure of a distribution network can be represented by a spanning tree *T* in the *G* if all root nodes are lumped together into one node. All the vertices in *G* are connected through a spanning tree *T* that does not contain any loop.

An example of the distribution network and the corresponding spanning tree representation is shown in Figure 15. After the occurrence of a fault, the out-of-service loads due to fault isolation should be restored by a sequence of switching operations. Isolating a line segment from the rest of the distribution network due to fault isolation requires opening of one or more (closed) sectionalizing switches. Switching operations during feeder restoration involve opening a normally closed sectionalizing switch and closing a normally open tie switch. Such a pair of switching operations guarantees that the radial network structure is maintained during the restoration process. Note that the switching operation pair corresponds to the cyclic interchange operation in graph theory. One cyclic interchange operation consists of adding an edge to the spanning tree to create a cycle and deleting another edge within this cycle. An example of cyclic interchange operations is shown in Figure 16. The spanning tree T_0 is transformed to spanning tree T_{d1} by deleting edge *d* and adding edge *b*. The spanning tree T_{d1} is further transformed to spanning tree T_{dh} by deleting edge *h* and adding edge *k*. If removing edge *d* in the spanning tree T_{d1} and T_{dh} indicates that branch 3-4 in the distribution newwork is de-energized due to fault isolation, the cyclic interchanges that transform spanning tree T_0 to T_{d1} and T_{dh} leads to candidate switching operations to restore out-of-service loads.

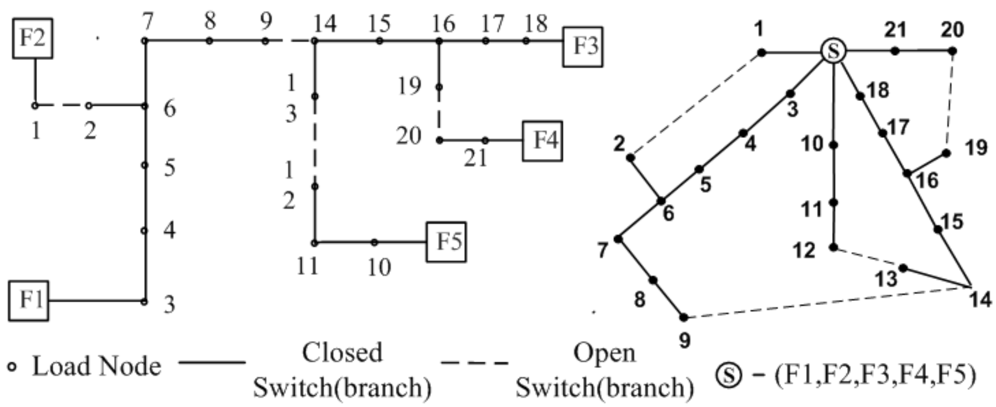

Figure 15. Spanning Tree Representation of Distribution Network Topology

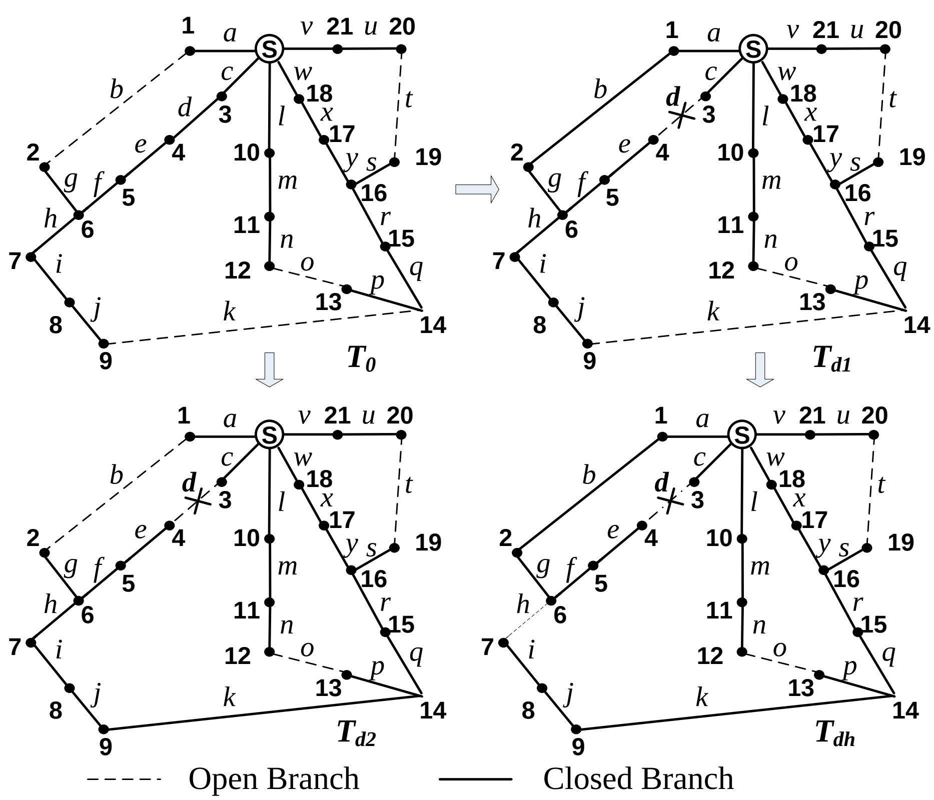

Figure 16. An Example of Spanning Tree Transformations

3.4.2 Generating Desired Spanning Trees for Distribution Restoration Problem

The distribution restoration problem consists of two major tasks: finding the final optimal network topology and providing a sequence of intermediate switching operations leading to this final network topology. If the pre-fault distribution network is represented by a spanning tree *T* in the graph *G*, these two tasks can be integrated as a combined task of finding the desired spanning tree *T'* in graph *G* and providing a sequence of cyclic interchange operations that transforms the initial spanning tree *T* to *T'*. An edge in *T* may be disconnected in *T',* which indicates that the corresponding branch in the original distribution network is de-energinzed by sectionalizing switches due to fault isolation.

A sequence of spanning trees can be generated with an increasing number of cyclic interchange operations sequentially without duplication using the algorithm presented in the previous section. The generated spanning trees respresent candidate distribution network topologies that could restore all the loads in the out-of-service areas. A computational procedure is illustrated with an example as follows.

The original distribution network is represented by a reference spanning tree T_0 as shown in Figure 16, where $T_0 = G - \{bkot\}$. Disconnecting the edge *d* of T_0 in Figure 15, a class of spanning trees T_d without edge *d* is calculated as follows:

Iteration 1) $T_d = \{t | t = T_0 \oplus \{de_i\}, e_i \in S_d(T_0), e_i \neq d\}$

$= \{T_{d1}, T_{d2}\} = \{G - \{dokt\}, G - \{dbot\}\}$, where $S_d(T_0) = \{dbk\}$.

Iteration 2) Replacing the edge *h* in T_{d1} *and* T_{d2}, a class of spanning trees T_{dh} are calculated as follows,

$T_{d1h} = \{t | t = T_{d1} \oplus \{he_i\}, e_i \in S_h(T_0) \cap S_h(T_{d1}), e_i \neq h\}$

$= \{G - \{dhot\}\}$, *where* $S_h(T_{d1}) = \{h,k\}$, $S_h(T_0) = \{h, k\}$.

$T_{d2h} = \{t | t = T_{d2} \oplus \{he_i\}, e_i \in S_h(T_0) \cap S_h(T_{d2}), e_i \neq h\}$

$= \{\Phi\}$, *where* $S_h(T_{d2}) = \{h,b\}$, $S_h(T_0) = \{h, k\}$.

It can be seen that spanning tree T_{dh} shown in Figure 16 is only transformed from T_{d1h}, the repeated generation from T_{d2h} is avoided.

The distribution network has a weakly meshed graph. The number of tie-switches in the distribution system is limited. It should be noticed that the total number of switching operation pairs required to restore the out-of-service load is equal to the number of cyclic interchange operations that transform the initial spanning tree to another spanning tree. This number is always less than or equal to the number of of tie-switches in the distribution system, depending on the electrical and operational constraints in the system.

3.4.3 Graph Simplification

The computation complexity for the spanning tree generation algorithms is strongly related to the total number of spanning trees N in the graph. To generate all the spanning trees of a graph $G = (V, E)$, the complexity of the algorithm described in section 3.3.2 is $O(|V||E|N)$. Since the number of spanning trees N will increase exponentially with the increasing number of vertices and edges, the computational burden can be significant for the above algorithm.

The computation complexity can be reduced substantially if the spanning tree generation algorithm is carried on a simplified graph, especially for a distribution system network [55]. For the distribution restoration problem, the output is a sequence of switching operations that correspond to the cyclic interchange operations between different spanning trees. In consequence, all the non-switch branches of the original distribution network can be removed. Moreover, the distribution network has a large number of degree one and degree two vertices. Such a network can be further simplified by removing some edges and vertices. The detailed graph simplification scheme is described below, and demonstrated with an example, as shown in Figure 17.

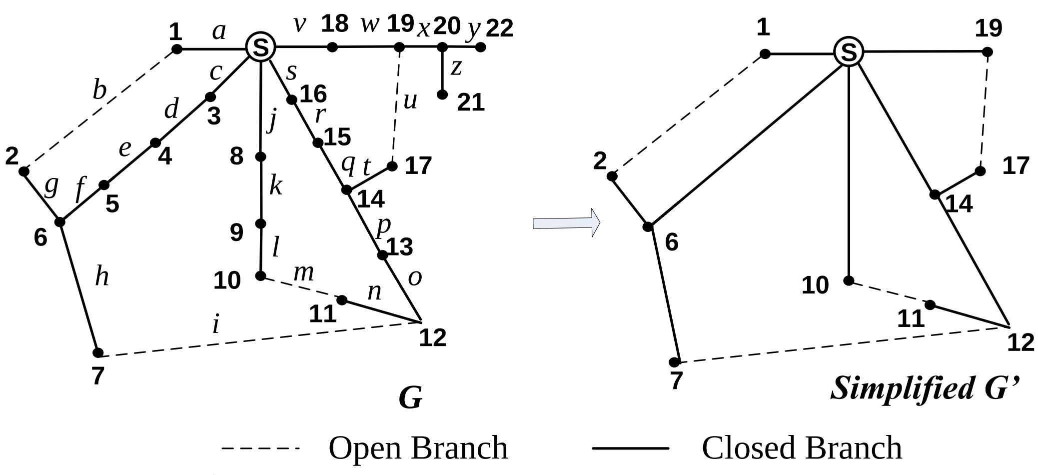

Figure 17. An Example of Graph Simplification

1) All the edges representing tie-switches and corresponding vertices connected are retained in the simplified graph.

2) All degree one vertices and the only edge connecting to it are removed recursively until there is no more degree one vertex in the graph. There is only one edge connecting to the degree one vertex. Removal of degree one vertices has no impact on the spanning tree generation. As shown in Figure 17, vertices 21, 22, 23 and edges *x*, *y*, *z* are removed.

3) Degree two vertices that are not connected to any edge representing tie-switch are removed. As shown in Figure 17, vertices 3, 4, 5 with degree two vertices are removed, and edges *c*, *d*, *e*, *f* connecting to these vertices are replaced with a single edge from node *S* to node 6.

It can be seen that the simplified graph will only contain closed loops. In a realistic distribution network, the number of branches and buses is large. After the graph simplification stage, the size of the graph can be reduced significantly. Before graph simplification, the converted graph of the test system applied in this paper has 1053 vertices and 1059 edges. After the simplification stage, the number of vertices and edges are reduced to only 19 and 25, respectively.

The candidate switching operations can be obtained by simply mapping the cyclic interchange operations on the simplified graph to the switching operations on the original distribution network. Since all the tie-switch branches are retained on the simplified graph, the adding an edge operation on the graph can be transferred to the closing corresponding tie-switch operation directly. The removing an edge operation on the graph can be transferred to the opening a sectionalizing switch operation. The candidate sectionalizing switch can be chosen from a corresponding set of sectionalizing switches. For example, as shown in Figure 17, removing the edge from node s to node 6 on the simplifed graph *G'* can be achieved by opening the sectionalizing switch on one of branches { *c*, *d*, *e*, *f*} on the graph *G*.

3.4.4 Proposed Distribution System Restoration Strategy

A two-phase strategy is proposed to meet the two objectives described in section 3.2. In the first phase, the network configuration with the minimum number of switching operations that can restore all of the load in the out-of-service area is searched sequentially. The spanning tree generation algorithm and the mapping technique described in the previous sections are applied to explore the potential network configurations. The candidate network topologies are recorded in terms of the switching operations that transform the original network topology to the new network topology. The three-phase unbalanced power flow calculation is applied to check if the electrical and operating constraints are met by the candidate network configuration. Starting from the first iteration, if no feasible network topology is found from a set of candidate network topologies, the next iteration will be triggerd. The iteration continues until a feasible solution is found or all the network topologies generated with the maximum number of switching operation pairs are explored. If a closing operation of a tie-switch resulted by the first iteration as well as opening operations of one or more sectionalizing switches due to fault isolation are considered as a switching operation pair, the number of iterations is equal to the number of switching operation pairs. The additional switching operation pairs resulted by the following iterations consist of several pairs of a closing operation of a tie-switch and an opening operation of a sectionalizing switch. The maximum possible number of switching operation pairs should be equal to or less than the total number of tie-switches in the system. If a feasible solution cannot be found to restore all the loads in the out-of-service area, a partial restoration strategy will be carried out in the second phase.

A sub-tree growth criteria is proposed to reduce the number of candidate network topologies, remove infeasible candidate network topologies, and avoid unnecessary power flow calulations, this criterion is illustrated in the following section. A flow chart of proposed algorithm is given in Figure 18. The iterative searching procedure is described as follows,

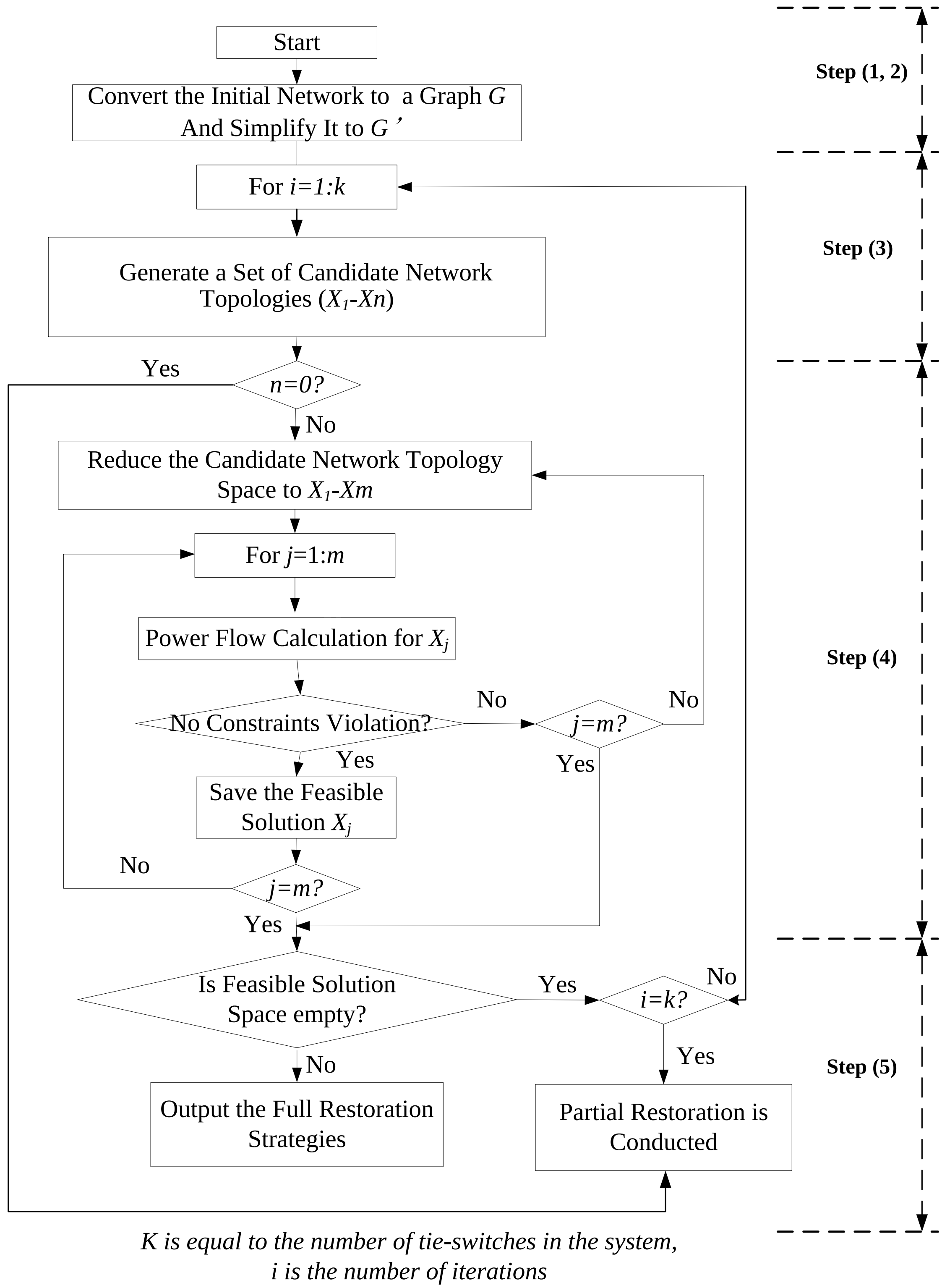

Figure 18. Proposed Distribution Restoration Algorithm

Step 1) Convert the distribution network to a graph *G*.

Step 2) Simplify the graph *G* to *G'*.

Step 3) A set of candidate network topologies is searched, starting from the first iteration. The new network configuration topologies in terms of the switching operations are mapped from the new spanning tree structure generated in the simplified graph *G'*. The spanning tree generation algorithm introduced in previous sections is applied to calculate the new spanning tree structure. In the simplified graph *G',*only the edges that represent tie-switches are open. The inserted edge in the newly formed spanning tree indicates a closing operation of a tie-switch. The deleted edge in the newly formed spanning tree indicates the openning operation of a sectionalizing switch. The radial structure is always maintained during the cyclic interchange operations.

Step 4) If the set of candidate network topologies obtained at the Step 3) is not empty, an unbalanced three-phase power flow is performed and constraints (i), (ii) and (iii) are checked for the candidate network configurations. If no constraint violation exists, the solution is saved as the feasible final configuration. Otherwise, some infeasible network configurations are removed in the solution list according to the criterion illustrated in the next section. After that, a three-phase power flow calulation is performed again to check the next candidate configuration in the solution list. The infeasible network configurations are checked and removed after every power flow calculation. If there is not a network configuration in the solution list that can restore all the loads in the out-of-service area, go to step 3) to find possible network configurations with an increased number of switching operations, the number of iterations *i* is added by one.

Step 5) If a solution satisfying all the electrical and operating constraints is found, output the result. If all of the potential network topologies are explored and there is not a configuration satisfying all the electrical and operation constraints, the partial load in the out-of-service area are selected to be restored. The minimum amount of load to relieve the overload is identified for the network topology with the least severe overload condition. Based on the previous power flow calculation results, if the lowest node voltage in the system is considered as the minimum node voltage for this network topology, then the network topology with the highest minimum node voltage is considered as the least severe overload topology.

The proposed distribution system restoration strategy explores the candidate network topologies to restore all loads in the out-of-service area starting from the minimum possible switching operations to the maximum possible switching operations. If a network topology that can restore all loads in the out-of-service area is found by the algorithm, the number of switching operations leading to this topology must be minimum.

3.4.5 A Sub-tree Growth Criterion to Reduce the Number of Candidate Topologies

In order to reduce the solution space, a sub-tree growth criterion is proposed. Each sub-tree connecting to the source node of the spanning tree represents a distribution feeder. The proposed criterion is inspired by the characteristics of the distribution power flow and the observation of the distribution taxonomy feeder model presented in the section 3.5.2. In this taxonomy feeder model, no inductive and capacitive load models are considered.

The proposed criterion is intended to restrict the growth of each sub-tree according to the power flow calculation results. An example to illustrate this criterion is shown in Figure 19. For the restoration scenario represented by a spanning tree transformation shown in Figure 16, the spanning tree T_{d1} is obtained by the first iteration. The switching operation that transforms T_0 to T_{d1} is to close the switch at edge *b* in Figure 16. The power flow calculation

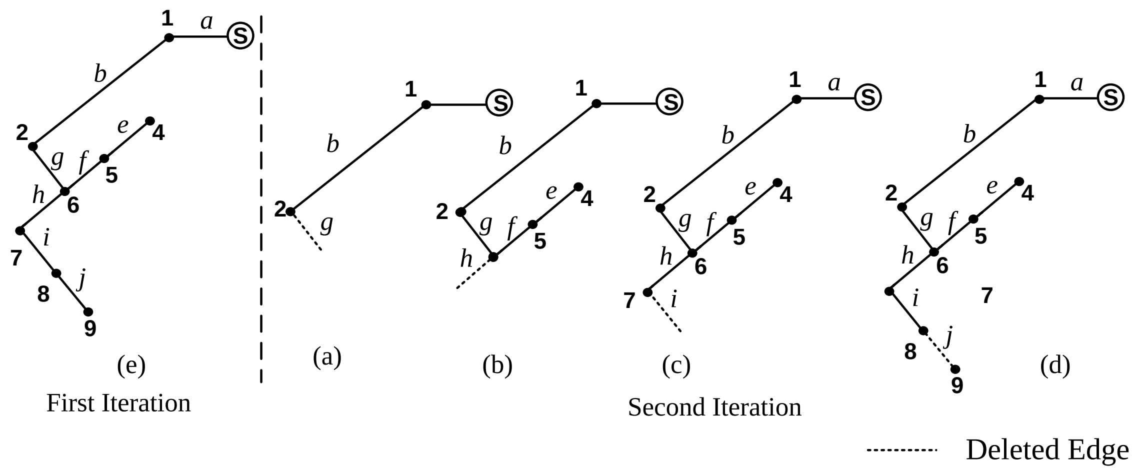

Figure 19. A Sub-tree Growth Example

results indicate that feeder 2 in Figure 15 is overloaded. A sub-tree starts from node s to node 9 in spanning tree T_{d1} that represents feeder 2 is shown in Figure 19. The second iteration is triggered to generate more spanning trees. The candidate switching operations leading to the new spanning trees are closing the switch at edge *k* and opening the switch at one edge selected from {*g, h, i, h*}. The sub-tree structure resulted from deleting edge *g, h, i,* or *j* is sub-tree (a) to sub-tree (d) as shown in Figure 19. It can be seen that the sub-tree grows from (a) to (e), where (a) has the shortest length. The longer sub-tree has a more severe overloading condition since more loads are connected to it. If there is a violation of electrical or operating constraints at sub-tree (a), the violation must exist at sub-tree (b) (c) (d) and (e).

The shortest length sub-tree has the highest priority for constraints checking. If there is a constraint violation at branch (a), the network topologies resulted from deleting edge *h, i* or *j* should be removed from the solution space.

In summary, the minimum length sub-tree structure that has an overloading condition in the system is recorded as a benchmark sub-tree structure, and updated after each power flow calculation. Each feeder in the candidate network topology has a corresponding benchmark sub-tree structure. Each sub-tree structure of the candidate network topology is compared with the corresponding benchmark sub-tree structure to determine the network topologies that cannot relieve the overloading condition. These network topologies are removed from the candidate topology list. According to this criterion, only the candidate network topologies that have the potential to alleviate the overload condition will be selected to check the constraints with power flow calculations. Therefore, unnecessary power flow calulations on the infeasible candidate network topologies can be avoided and the computation speed can be increased.

3.4.6 Optimality and Complexity of the Proposed Algorithm

An optimal network topology is the one which, among all possible network topologies, has the minimum number of switching operations that transforms the system configuration after the fault to the post-restoration configuration. The proposed algorithm applies the spanning tree search algorithm to generate every possible network topology to restore all out-of-service loads. Starting from a pair of switching operations, a sequence of candidate network topologies are generated with increasing number of switching operations.

If a network topology satisfying the electrical and operating constraints is found by constraints checking, such a network topology must be optimal. Because all the possible network topologies with fewer switching operations have been explored, and their infeasibility with respect to the constraints have been verified. However, such an optimal configuration may not exist. If such an optimal network topology can not be found, a partial restoration configuration will be pursued instead.

The complexity of the proposed algorthm depends on the efficiency of spanning tree search algorithm, the number of spanning trees searched, and the number of spanning tree stuctures that should be applied to check the constraints by power flows. Generating one spanning tree structure that could restore all out-of-service loads requres the order of $O(|V||E|)$ in computation time. The complexity of generating spanning trees is reduced by generating the desired spanning trees on a significantly simplified graph for a weakly meshed graph [55]. The number of spanning tree configurations that are required for power flow calculation is further reduced with the proposed sub-tree growth criterion introduced in section 3.4.5.

3.5 Test System and Simulation Environment

3.5.1 GridLAB-D Simulation Environment

The proposed graph theoretic distribution restoration strategy is implemented and tested in the GridLAB-D environment. GridLAB-D [56] is a new power system modeling and simulation environment developed by the U.S. Department of Energy at Pacific Northwest National Laboratory (PNNL) for the study of power distribution systems and the smart grid technologies with detailed end-use and power distribution automation models. GridLAB-D has an advanced algorithm that can determine the simultaneous state of millions of independent devices. Hence, GridLAB-D does not require the use of reduced-order models, which avoid the danger of erroneous assumptions.

The proposed algorithm is implemented with *C++* under the GridLAB-D environment. The simulation results are obtained on a PC with an Intel Core 2.8 G CPU and 3.8 G RAM.

3.5.2 Taxonomy Feeder Models in GridLAB-D

A set of radial distribution test feeders representing those found in various regions in the Continental United States with a GridLAB-D compatible format has been created and reported [57]. These taxonomy feeder models with detailed load models represent realistic distribution feeders in U.S. utilities. Each feeder model contains all detailed system elements from the generator, substation regulator, distribution lines to the end-use meters. Each feeder model was designed to represent a specific voltage level and load composition within the various climate regions of the United States.

A multi-feeder test system consisting of four taxonomy feeder R3-12.47-2 [57] that is a representation of a moderately populated urban area is created. This feeder is composed of single family homes, light commercial loads, and a small amount of light industrial loads. The test system has a GridLAB-d compatible format, with a detailed network model and a combination of constant power, constant current, and constant impedance load models. In this multi-feeder system, feeders are connected to adjacent feeders through 7 normally open tie-switches. There are 1053 nodes and 1059 branches in this system. The voltage level for this system is 12.47 kV. Detailed information about the number of components is shown in Table 5. The simplified one-line diagram is shown in Figure 20. This system is assumed to be in a peak load condition. The minimum node voltage in this system is 259.698V, which is 93.72% of the nominal node voltage that is 277.1 V.

Table 5. 1053 Node Four Feeder Test System

# of Nodes	1053	Load (kVar)	2361.818
# of Tie Switches	7	# of Load Nodes	248
# of Sectionalizing Switches	164	# of Commercial Transformers	228
Load (kW)	17467.82	# of Industrial Transformers	21

3.5.3 Distribution Power Flow in GridLAB-D

GridLAB-D has two modules that are able to perform power flow calculations at both the transmission and the distribution levels. While distribution systems are the primary focus of GridLAB-D, the transmission module is included so that the interactions between two or more distribution systems can be simulated [58]. Hence, it has the ability to calculate the power flow solution for multiple distribution systems interconnected via a transmission or sub-transmission network.

The algorithm for power flow calculations at the transmission level is the Gauss-Seidel (GS) method. To solve the unbalanced three-phase power flow on the distribution level, three different algorithms including the traditional forward and backward sweep method, the Gauss-Seidel (GS) method and the Newton Raphson (NR) method [58] are implemented in GridLAB-D.

The components of a distribution system that are implemented and available for use in GridLAB-D include overhead and underground lines, transformers, voltage regulators, fuses, switches, and shunt capacitor banks.

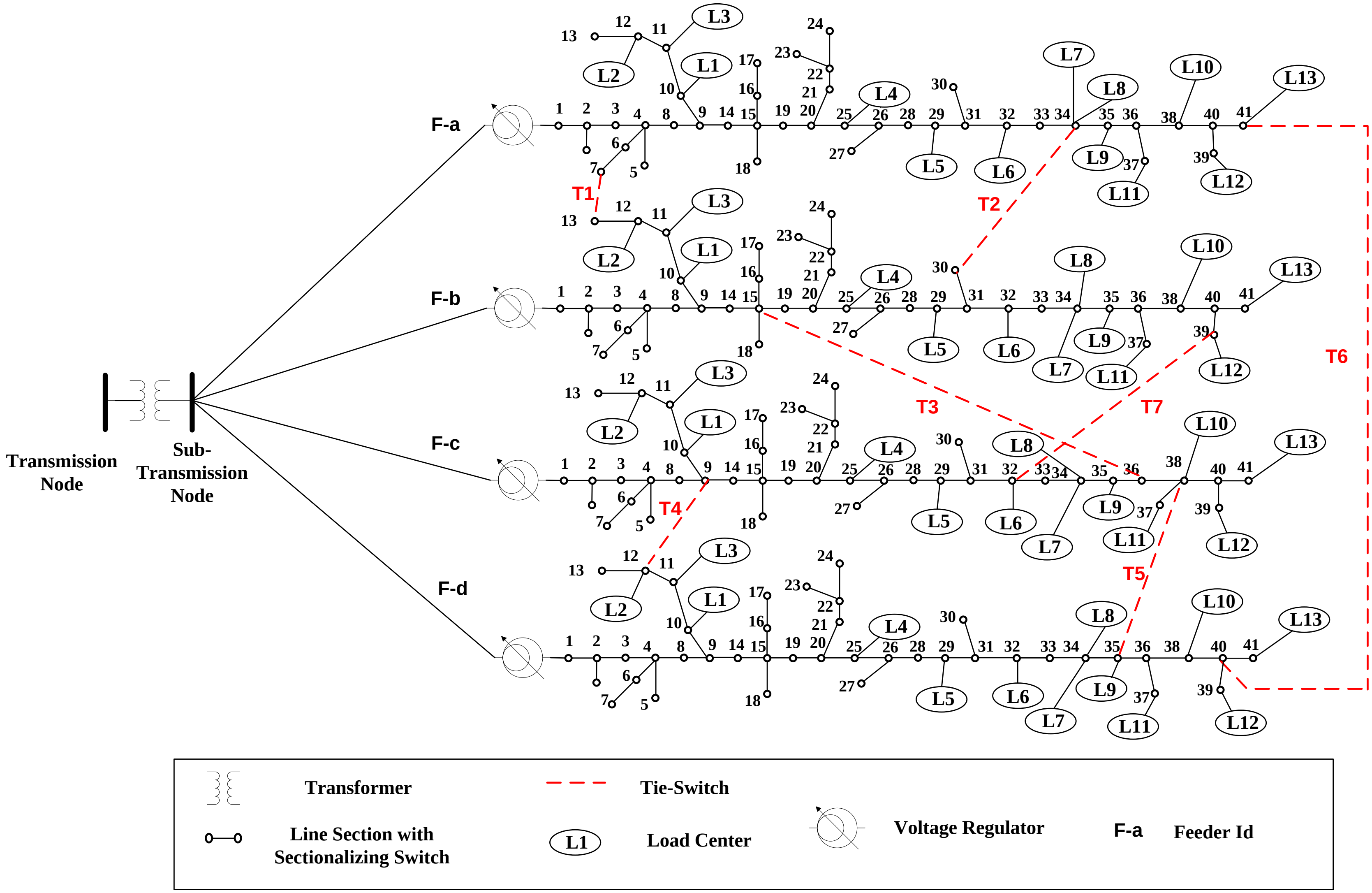

Figure 20. A Simplified One-Line Diagram of the Four-Feeder 1060 Nodes Distribution System

3.6 Numerical Results

3.6.1 Full Load Restoration

Table 6 provides four full load restoration scenarios.

Table 6. A Sequence of Switching Operations of Full Load Restoration

Scenario 1	Fault Location : (F-b-39 and F-b-40)			
	# Unsupported Node: 8		# Switching Operations: 1	
Sequence:	Close	T7		
Scenario 2	Fault Location : (F-c-36 and F-c-38)			
	# Unsupported Node: 18		# Switching Operations: 3	
Sequence:	Close	T5		
	Open	F-d-38 and F-d-40	Close	T6
Scenario 3	Fault Location : (F-d-34 and F-d-35)			
	# Unsupported Node: 112		# Switching Operations: 5	
Sequence:	Open	F-d-38 and F-d-40		
	Close	T5	Close	T6
	Open	F-c-35 and F-c-36	Close	T3
Scenario 4	Fault Location : (F-a-31 and F-a-32)			
	# Unsupported Node: 146		# Switching Operations: 7	
Sequence:	Open	F-a-36 and F-a-38		
	Close	T2	Close	T6
	Open	F-b-36 and F-b-38	Close	T7
	Open	F-d-11 and F-d-12	Close	T4

It is assumed that the faulted line is isolated by switching off the sectionalizing switches on both sides of the line. A sequence of switching operations generated by the proposed algorithm is able to restore all the loads in the out-of-service area for these four scenarios. The acceptable minimum node voltage after the system restoration in the algorithm is set to be 257.7 V, which is 93% of the nominal voltage. The power flow calculations are performed to assure that the post-restoration system will not violate the line current, node voltage or transformer capacity constraints. In the four restoration scenarios, only node voltage constraints are violated by some of candidate system topologies. The simulation time for the four scenarios shown in Table 6 is 6s, 7s, 17s, and 39s, respectively.

In scenario 1, the system is restored by closing tie-switch T7.The minimum node voltage in the post-restoration system is 259.1 V, which is 93.52% of the nominal node voltage.

In scenario 2, the system is restored by closing two tie-switches, opening one sectionalizing switch following the operation sequence in Table II. This scenario is identical to the “load transfer” scenario in [19]. Some nodes in the system after a closing operation of a tie-switch violate the node voltage constraint. The system is overloaded by connecting all the load in the out-of-service area to feeder F-d, and the overload condition is alleviated by a load transfer operation. Partial loads are transferred from feeder F-d to feeder F-a by a switching operations pair. The minimum node voltage in the post-restoration system is 258.78 V, which is 93.39% of the nominal node voltage.

In scenario 3, 5 switching operations including closing three tie-switches and opening two sectionalizing switches in Table 6 are identified by the proposed algorithm. The node voltage constraint is violated in the system obtained after only 1 or 3 switching operations. This scenario is a combination of the “zone restoration [19]” and the “load transfer [19]” scenario. The out-of-service area is separated into two zones by opening sectionalizing switch between node F-d-38 and F-d-40 first, then these two load zones are restored by closing tie-switch T5 and T6. After that, some load in feeder F-c are transferred to feeder F-b by opening sectionalizing switch F-c-35 and F-c-36 and closing tie-switch T3 to relieve the overload condition at feeder F-c. The minimum node voltage in the post-restoration system is 258.31 V, which is 93.22% of the nominal node voltage.

Scenario 4 is a more complicated restoration scenario, where 7 switching operations shown in Table 6 are required to reach the final post-restoration configuration. There are one “zone restoration” and two times “load transfer” in this scenario. In the evolutionary restoration process, the minimum node voltage is gradually increasing at each restoration stage, as shown in Figure 21. After the first three switching operations, the out-of-service area is separated into two zones, and these two zones are connected to feeder F-b and feeder F-d, respectively. Both feeder F-b and feeder F-d are overloaded after the “zone restoration”. Consequently, two more switching operation pairs are suggested to transfer load from feeder F-b to F-c, and from F-d to F-c. The minimum node voltage in the final post-restoration system is 258.03 V, which is 93.12% of the nominal node voltage.

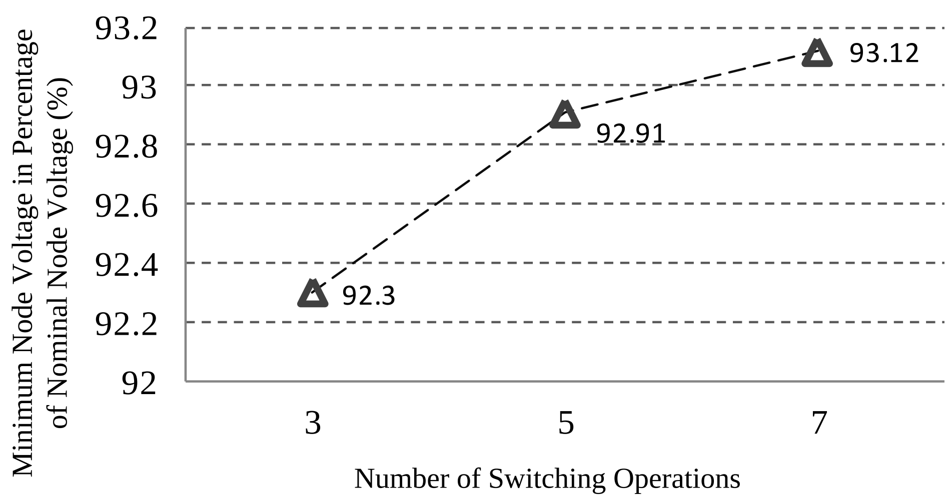

Figure 21. The Evolution of Minimum Node Voltage in Scenario 4

3.6.1 Partial Load Restoration

If the minimum allowed node voltage is increased from 257.7 V to 259.08 V, which is increased from 93% to 93.5% of the nominal node voltage. A full load restoration strategy cannot be found by the proposed algorithm. Since the node voltage constraint is only violated at node F-c-40 and F-c-41 in the post-restoration system of scenario 4. After disconnecting some of loads in load center L13 at feeder F-c, the system is restored by picking up as much load as possible without violations of the constraints.

3.7 Summary

The distribution system restoration is aimed at restoring loads after a fault by altering the topological structure of the distribution network while meeting electrical and operational constraints. Such a network reconfiguration process is usually achieved by changing open/closed states of some tie switches and sectionalizing switches in the distribution system. This chapter presents a graph-theoretic distribution restoration strategy that maximizes the amount of load to be restored and minimizes the number of switching operations. Spanning tree based algorithms are applied to find the candidate restoration strategies. Unbalanced three-phase power flow calculation is performed to help reduce the solution space. Simulation results obtained from realistic feeder models demonstrate the effectiveness of the proposed approach.

CHAPTER 4. CONCLUSIONS AND FUTURE WORK

4.1 Conclusions

The main results of this research are two graph-theoretic algorithms for controlled area partitioning at the transmission level and feeder restoration at the distribution level. This research is motivated by recent development of the “smart grid” vision to modernize the grid infrastructure and support “self-healing” feature for both transmission and distribution networks.

The proposed self-healing power system reconfiguration algorithm minimizes both real and reactive power imbalance between generation and load. Dynamic simulations on a 200-bus system verify that the voltage profile after the system reconfiguration determined by the proposed algorithm is much improved compared with the result of an algorithm that only considers real power balance. Simulation results on a 22,000-bus system demonstrate that the proposed algorithm is highly efficient computationally. The feasibility to apply the proposed area partitioning algorithm as an emergency control system is established.

The proposed graph-theoretic distribution restoration algorithm applies the spanning tree search technique in graph theory to find the network topologies are capable of picking up all out-of-service loads. The cyclic interchange operations that transform spanning trees represent the necessary remedial switching actions transforming the initial post-fault system topology into the final system topology. Power flow calculations with detailed network model are performed to ensure that the network topologies suggested by the proposed algorithm will be operated within the electrical and operation limits. An optimal solution, that is a restoration plan with minimum switching operations for a full-load restoration, can be identified by the proposed algorithm. In case the system is highly overloaded and no feasible network topology that can restore all out-of-service loads exists, a restoration plan that picks up as much load as possible without violations of the constraints is suggested. The execution time for a 1053 node realistic multi-feeder system is in the order of seconds, which indicates that it is promising to apply the approach to realistic distribution systems for restoration planning or operation.

4.2 Future Work

With the growing needs of renewable energy and increasing penetration of distributed generations, a self-healing smart grid is desirable in the future. Such a smart grid should have the capabilities of wide-area situational awareness, grid monitoring on a real-time basis and early warning that recognizes vulnerable operating conditions in a timely manner. Hence, this smart grid allows the system to take preventive and corrective control actions automatically in response to vulnerable operating conditions. The deployment of PMUs and high bandwidth communications enhance the technical feasibility of a smart grid [59]. Although significant progress has been made in this research, the following important issues remain to be addressed in the future:

1. The proposed partitioning algorithm presented in Chapter 2 can be combined with a load shedding scheme to achieve a smart grid technology that enhances robustness of the system and minimizes the impact of cascading events. Moreover, post-islanding controls, such as automatic capacitor switching and automatic generation control, should be developed to further stabilize the islands formed by system reconfiguration. An automatic defense

system scheme that integrates area partitioning operations, load shedding and post-islanding control actions is desirable.

2. A self-healing transmission network should be able to predict cascading events, evaluate system vulnerability, than trigger immediate automatic control actions in times of crisis. The intentional area partitioning scheme is one of remedial control actions to prevent or mitigate catastrophic outages. Fast dynamic simulation tools and large scale deployment of PMUs are expected to enable the real time wide-area situational awareness to anticipate vulnerable operating conditions. Some basic patterns of cascaded events are investigated in Chapter 2. More efforts should be made to identify the vulnerable operating conditions of power grids based on pattern analysis, and determine the time to trigger emergency controls with the system vulnerability information.

3. Quickly activating the spinning reserves of generators would help to restore the post-islanding system to its normal operating frequency. The proposed partitioning algorithm presented in Chapter 2 does not consider the spinning reserves. The effect of spinning reserve control in the intentional system islanding should be investigated.

4. It is a major task to construct the infrastructures needed for implementation of the on-line system reconfiguration scheme. Although a conceptual relaying system for controlled system reconfiguration is envisioned in Chapter 2, the design of this system is still at an early stage. A comprehensive and detailed relaying system together with a communication system dealing with the actual system reconfiguration control actions should be investigated.

5. The distribution scenarios presented in Chapter 3 are all dealing with a single fault scenario. In a real situation, simultaneous multiple faults resulting more than two areas

disconnected from the grid may happen under severe weather conditions. The proposed spanning tree search algorithm has the capability to find the network topologies that connect all the out-of-service areas to the system regardless of the total number of these areas. More research should be conducted to evaluate the performance and efficiency of the proposed algorithm to handle multiple faults.

6. The proposed spanning search algorithm is intended to find the distribution network topology with a radial structure. Improvements should be made for the proposed algorithm to apply it on a weakly meshed distribution network.

7. In the four restoration scenarios presented in Chapter 3, only low voltages that violate node voltage constraints occur in some of candidate system topologies. Switching on capacitor controls can improve the low voltage profile in the system. An extension of proposed distribution restoration algorithm is to formulate the distribution restoration problem considering capacitor controls.

8. In the proposed distribution system restoration strategy, load models considered are constant current, power and impedance loads. During a normal operation condition, load changes constantly. It is important to take load variations into consideration in the distribution restoration planning. It is desirable to investigate how to build a proper stochastic load model that could represent the load variations.

9. Advances in distributed generation (DG) technologies are providing an opportunity for increased penetration of DGs within a power distribution system, which will have an impact on distribution restoration. A traditional distribution restoration plan that assumes a single power source (substation) for each customer may not be appropriate for the distribution system with DGs. It is desirable to analyze the impact of location and capacity

sizing of DGs during distribution system restoration. A new distribution restoration strategy considering DGs should be developed.

10. Today, distribution system restoration is commonly performed by dispatching field crews to manually operate switches on site. The distribution automation system is only applied at a local level at the substations. Simulation results shown in Chapter 3 demonstrate that the system-wide switching operations have better performance than the switching operations at a local level in terms of alleviating the system overload condition. Automated system-wide switching operations among multiple feeders are expected in the future distribution restoration system to minimize outages and enhance system reliability. In order to achieve such an advanced distribution restoration system, a revolutionary infrastructure for distribution system monitoring, communication and controls will be needed. An advanced communication network with a high bandwidth, more redundancy, less latency and better compatibility will need to be developed to enable the change of power industry towards the smart grid at the distribution level.

4.3 List of Publications

J. Li, C. C. Liu and K. Schneider, "Controlled Partitioning of a Power Network Considering Real and Reactive Power Balance," Accepted for publication in *IEEE Trans. Smart Grids*, 2010.

J. Li, C. C. Liu, K. Schneider, and G. Manimaran, "Distribution System Restoration Based on Graph Theoretic Algorithms," To be Submitted to *IEEE Trans*. *Power Delivery*.

K. Yamashita, S.K. Joo, **J. Li**, P. Zhang, and C. C. Liu, "Analysis, Control, and Economic Impact Assessment of Major Blackout Events," *European Transactions on Electrical Power*, vol. 18, no. 8, pp. 854-871, Nov 2008.

K.Yamashita, **J. Li**, C. C. Liu, and P. Zhang, "Learning to Recognize Vulnerable Patterns Due to Undesirable Zone-3 Relay Operations", *IEEJ Transactions on Electrical and Electronic Engineering*, Vol.4 No.3, 2009, pp.322-333.

J. Li and C. C. Liu, "Power System Reconfiguration Based on Multilevel Graph Partitioning," *Proceedings of the 2009 PowerTech Conference*, Bucharest, Romania, June, 2009.

J. Li, K. Yamashita, C. C. Liu, P. Zhang, and M. N. Hofmann, "Identification of cascaded generator over-excitation tripping events," *Proceedings of 16th Power Systems Computation*

Conference, Glasgow, Scotland, 2008.

C. C. Liu and **J. Li**, “Patterns of Cascaded Events,” *Proceedings of IEEE PES General Meeting*, July 2009.

K. Yamashita, **J. Li**, P. Zhang, and C. C. Liu, "Analysis and Control of Major Blackout Events," *Proceedings of 2009 IEEE PES Power System Conference & Exhibition (PSCE)*, March 2009, USA.

BIBLIOGRAPHY

[1] "Grid 2030: A National Version for Electricity's Second 100 Years", Office of Electric Transmission and Distribution, United State Department of Energy, July 2003.

[2] NIST Framework and Roadmap for Smart Grid Interoperability Standards, Release 1.0, [Online]. Available: http://www.nist.gov/public_affairs/releases/upload/smartgrid_interoperability_final.pdf.

[3] Anticipates and Responds to System Disturbances (Self-Heals), National Energy Technology Laboratory, Release 2.0, [Online]. Available: www.netl.doe.gov/.../09.02.2010_Anticipates%20and%20Responds%20(Self%20Heals).pdf

[4] J. Yan and C.C. Liu, "Application of Phasor Measurement Units (PMUs) Data for Monitoring of System Dynamics in the On-Line Environment," Electric Power Research Center (EPRC) Report, 2009.

[5] B. Milosevic and M. Begovic, "Voltage-Stability Protection and Control Using a Wide Area Network of Phasor Measurements," *IEEE Trans. Power Systems*, vol. 18, no. 1, pp. 121–127, Feb. 2003.

[6] CIGRE Technical Brochure on "Wide Area Monitoring and Control for Transmission Capability Enhancement," Working Group 610 of Study Committee C4, Final Report, Jan. 2007.

[7] H. Li, G. Rosenwald, J. Jung, and C. C. Liu "Strategic Power Infrastructure Defense," *Proceedings of the IEEE*, vol. 93, no. 5, pp. 918–933, May 2005.

[8] P. Anderson and B.K. LeReverend, "Industry Experience with Special Protection Schemes," *IEEE Trans. Power Systems*, vol. 11, no. 3, pp. 1166-1179, Aug. 1996.

[9] B. A. Archer and J. B. Davies, "System Islanding Considerations for Improving Power System Restoration at Manitoba Hydro," IEEE Canadian Conference on Electrical and Computer Engineering (CCECE 2002), vol 1, pp. 60-65.

[10] Y. V. Makarov, V. I. Reshetov, V. A. Stroev, and N. I. Voropai, "Blackout Prevention in the United States, Europe, and Russia," *Proceedings of the IEEE*, vol. 93, No. 11, pp. 1942–1955, Nov. 2005.

[11] J. Jung, C. C. Liu, S. L. Tanimoto, and V. Vittal, "Adaptation in Load Shedding Under Vulnerable Operating Conditions," *IEEE Trans. Power Systems*, Vol. 17, No. 4, pp. 1199-1205, Nov. 2002.

[12] K. Moslehi and R. Kumar, "Smart Grid – A Reliability Perspective", IEEE PES Conference on "Innovative Smart Grid Technologies", Washington DC, Jan. 2010.

[13] B. Yang, V. Vittal, and G. T. Heydt, "Slow Coherency Based Controlled Islanding – A Demonstration of the Approach on the August 14, 2003 Blackout Scenario," *IEEE Trans. Power Systems*, vol. 21, No. 4, pp.1840-1847, Nov. 2006.

[14] K. Sun, D. Zheng, and Q. Lu, "Splitting Strategies for Islanding Operation of Large-scale Power Systems Using OBDD-Based Methods," *IEEE Trans. Power Systems*, vol. 18, no. 2, pp. 912-923, May 2003.

[15] H. You, V. Vittal, and X. Wang, "Slow Coherency-Based Islanding," *IEEE Trans. Power Systems*, vol. 19, no. 1, pp. 483–491, Feb. 2004.

[16] X.Wang and V.Vittal, "System Islanding Using Minimal Cutsets with Minimum Net Flow," *Proceedings of the 2004 IEEE PES Power System Conference and Exposition*, New York, October, 2004.

[17] B. Yang, "Slow Coherency Based Graph Theoretic Islanding Strategy," Ph.D. Dissertation, Arizona State University, 2007.

[18] G. Xu and V. Vittal "Slow Coherency Based Cutset Determination Algorithm for Large Power Systems," *IEEE Trans. Power Systems*, vol. 25, No. 2, pp.877-884, May 2010.

[19] C. C. Liu, S. J. Lee, and S. S. Venkata, "An Expert System Operational Aid for Restoration and Loss Reduction of Distribution Systems," *IEEE Trans. Power Systems*, vol. 3, no. 2, pp. 619–626, May 1988.

[20] K. Aoki, K. Nara, M. Itoh, et al., "A New Algorithm for Service Restoration in Distribution Systems," *IEEE Trans. Power Delivery*, Vol. 4, No. 3, July 1989, pp. 1832-1839.

[21] Y. Y. Hsu and H. C. Kuo, "A Heuristic Based Fuzzy Reasoning Approach For Distribution System Service Restoration," *IEEE Trans. Power Delivery*, Vol. 9, No. 2, April 1994, pp. 948-953.

[22] Y. Fukuyama, H. D. Chiang, and K. N. Miu, "Parallel Genetic Algorithm for Service Restoration in Electric Power Distribution Systems," *Electric Power & Energy Systems*, Vol. 18, No. 2, 1996, pp. 111-119.

[23] Q. Zhou, D. Shirmobammadi, and W. H. Liu "Distribution Feeder Reconfiguration For Service Restoration and Load Balancing," *IEEE Trans. Power Systems*, Vol. 12, No. 2, May 1997, pp. 724-729.

[24] S. J. Lee, S. I. Lim, and B. S. Ahn, "Service Restoration of Primary Distribution Systems Based on Fuzzy Evaluation of Multi-Criteria," *IEEE Trans. Power Systems*, vol. 13, pp. 1156–1163, Aug. 1998.

[25] K. N. Miu, H. D. Chiang, B. Yuan, and G. Darling, "Multi-Tier Restoration Through Network Reconfiguration and Capacitor Control for Large-Scale Radial Distribution Network," *IEEE Trans. Power Systems*, vol. 15, no. 3, Aug. 2000, pp. 1001–1007.

[26] C. S. Chen, C. H. Lin, and H. Y. Tsai, "A Rule-Based Expert System with Colored Petri Net Models for Distribution System Service Restoration," *IEEE Trans. Power Systems*, vol. 17, no. 4, pp. 1073-1080, Nov. 2002.

[27] Y. T. Hsiao and C. Y. Chien, "Enhancement of Restoration Service in Distribution System using a Combination Fuzzy-GA Method," *IEEE Trans. Power Systems*, vol. 15, pp. 1394–1400, Nov. 2000.

[28] T. Nagata and H. Sasaki, "A Multi-agent Approach to Power System Restoration," *IEEE Trans. Power Systens*, vol. 17, no. 2, pp. 457–462, May. 2002.

[29] S. Lim, S. J. Lee, M. S. Choi, D. J. Lim, and B. N. Hua, "Service Restoration Methodology for Multiple Fault Case in Distribution Systems," *IEEE Trans. Power Systems*, vol. 21, no. 4, pp. 1638–1644, Nov. 2006.

[30] M. S. Tsai, "Development of an Object-Oriented Service Restoration Expert System With Load Variations," *IEEE Trans. Power Systems*, vol. 23, pp. 219–225, Feb.2008.

[31] P M S Carvalho, L A F M Ferreira, and L M F Barruncho, "Optimization Approach to Dynamic Restoration of Distribution Systems," *Inter. Journal of Electrical Power & Energy Systems*, Vol. 29, Issue 3, pp. 222-229, March 2007.

[32] R. E. Pérez-Guerrero and G. T. Heydt, "Optimal Restoration of Distribution Systems using Dynamic Programming," *IEEE Trans. Power Delivery*, vol. 23, no. 3, pp. 1589–1596, July 2007.

[33] R. E. Pérez-Guerrero and G. T. Heydt, "Distribution System Restoration via Subgradient based Lagrangian Relaxation," *IEEE Trans. Power Systems*, vol. 23, no. 3, pp. 1162-1169, Aug. 2008.

[34] W. Sun, C. C. Liu, and R. F. Chu, "Optimal Generator Start-Up Strategy for Power System Restoration, " *Procedings of ISAP*, Brazil, 2009.

[35] V. Venkatasubramanian and Y. Li, "Analysis of 1996 western American electric blackouts," *Proc. Bulk Power System Dynamics and Control VI Conf.*, Cortina, Italy, 2004.

[36] U.S.-Canada Power System Outage Task Force, "Final Report on the August 14th blackout in the United States and Canada," United States Department of Energy and National Resources Canada, April 2004. [Online] available: https://reports.energy.gov/BlackoutFinal-Web.pdf

[37] UCTE, "Final Report of the Investigation Committee on the 28 September 2003 Blackout in Italy," April 2004. [Online] available: http://www.ucte.org/_library/otherreports/20040427_UCTE_IC_Final_report.pdf

[38] UCTE, "Final Report on the Disturbances of 4 November 2006," Jan. 2007. [Online] available: http://www.ucte.org/_library/otherreports/Final-Report-20070130.pdf

[39] P. Pourbeik, P.S. Kundur, and C. W. Taylor, "The Anatomy of a Power Grid Blackout - Root Causes and Dynamics of Recent Major Blackouts," *IEEE Power and Energy Magazine*, pp. 22-29, April 2006.

[40] I. Dobson, B.A. Carreras, V. Lynch, D.E. Newman, "Complex systems analysis of series of blackouts: cascading failure, criticality, and self-organization," Bulk Power System Dynamics and Control VI Conf., Cortina, Italy, 2004.

[41] WSCC, "Western Systems Coordinating Council (WSCC) Disturbance Report for the Power System Outage that Occurred on the Western Interconnection, August 10, 1996," Approved by the WSCC Operations Committee on October 18, 1996.

[42] P. Anderson and B.K. LeReverend, "Industry Experience with Special Protection Schemes," *IEEE Trans. Power Systems*, vol. 11, no. 3, pp. 1166-1179, Aug. 1996.

[43] K. Schloegel, G. Karypis, and V. Kumar, "A New Algorithm for Multiobjective Graph Partitioning," *Proc. EuroPar*, Toulouse, France, pp. 322–331. 1999.

[44] G. Karypis and V. Kumar, "A Fast and High Quality Multilevel Scheme for Partitioning Irregular Graphs," *SIAM Journal on Scientific Computing*, vol.20, no. 1, pp. 359-392, 1998.

[45] J. Li and C.C. Liu, "Power System Reconfiguration Based on Multilevel Graph Partitioning," *Proceedings of 2009 PowerTech*, Bucharest, Romania, June 2009.

[46] M. Begovic, D. Novosel, D. Karlsson, C. Henville, and G. Michel, "Wide-Area Protection and Emergency Control," *Proeedings of the IEEE*, vol. 93, pp. 876-891, May 2005.

[47] K. Yamashita, S. K. Joo, J. Li, P. Zhang, and C. C. Liu, "Analysis, Control and Economic Impact Assessment of Major Blackout Events," *European Trans. Electrical Power*, pp. 854-871, Nov. 2008.

[48] N. Senroy, G. T. Heydt, and V .Vittal, "Decision Tree Assisted Controlled Islanding," *IEEE Trans. Power Systems*, Vol. 21, No. 4, pp. 1790-1797, Nov. 2006.

[49] IEEE PSRC WG D6 Report, "Power Swing and Out-Of-Step Considerations on Transmission Lines," July 2005.

[50] C. W. Taylor, D. C. Erickson, K. E. Martin, R. E. Wilson, and V. Venkatasubramanian, "WACS-Wide Area Stability and Voltage Control System: R&D and online demonstration," *Proceedings of the IEEE*, (*Special Issue on Energy Infrastructure and Defense Systems*), Vol. 93, No. 5, May 2005.

[51] ANSI C50.13-1977 - ANSI National Standard Requirements for Cylinderical Rotor Synchronous Generators, 1977.

[52] Willis, H. L., *Power Distribution Planning Reference Book*, Marcel Dekker, Inc., 2nd ed., 2004

[53] N. Deo, *Graph Theory with Application to Engineering and Computer Science*.

Englewood Cliffs, NJ: Prentice-Hall, 1974.

[54] W. Mayeda and S. Seshu, "Generation of Trees without Duplications," *IEEE Trans. Circuit Theory*, vol. 12, no. 2, pp. 181-185, Jun. 1965.

[55] N. S. Bhagat, "Efficient Spanning Tree Enumeration Using Loop Domain," *IEEE Systems Journal*, vol. 3, no. 4, pp. 536-543, Dec. 2009.

[56] U.S. Department of Energy at Pacific Northwest National Laboratory. GridLAB-D, power distribution simulation software. [Online] available: www.gridlabd.org

[57] K. P. Schneider, Y. Chen, D. Engle, and D. Chassin, "A Taxonomy of North American Radial Distribution Feeders," *Proceedings of IEEE PES General Meeting*, Minneapolis, July. 2009.

[58] K. P. Schneider, D. P. Chassin, Y. Chen, and J. C. Fuller, "Distribution Power Flow for Smart Grid Technologies," *Proceedings of IEEE Power System Conference and Exposition*, Seattle, WA, March 2009.

[59] A. Bose, "Smart Transmission Grid Applications and Their Supporting Infrastructure," *IEEE Trans. Smart Grid*, vol. 1, No. 1, pp.11-19, June 2010.